Chapter 5
Radiation-Enhanced Diffusion and Defect Reaction Rate Theory

We have developed an understanding of the formation of point defects, their motion or diffusion in a solid, and the configurations of some of the common types of defect clusters encountered in irradiated and unirradiated metals. Clearly, the formation, growth, and dissolution of defect aggregates such as voids, dislocation loops, etc., depend upon the diffusion of point defects and their reaction with the defect aggregates. But they also depend upon the concentration of point defects in the solid. The concentration at any point and time is a balance between the production rate and the loss rate of point defects and is adequately described by the *point defect balance equations*. The increase in diffusion or enhancement of atom mobility in an irradiated metal is due to two factors: (1) the enhanced concentration of the defects and (2) the creation of new defect species.

Recall that the diffusion of lattice atoms by way of the vacancy mechanism is given by:

$$D_a^v = f_v D_v C_v,$$

where D_v is the vacancy diffusion coefficient, C_v is the vacancy concentration, and f_v is the correlation coefficient. Thus, increasing the concentration of vacancies will increase the diffusion coefficient for the atoms in the metal. However, if other mechanisms of diffusion are operative, such as interstitials or divacancies, then the total diffusion coefficient for atoms, D_a is written as follows:

$$D_a = f_v D_v C_v + f_i D_i C_i + f_{2v} D_{2v} C_{2v} + \cdots$$

and diffusion of atoms in the metal is increased by opening new channels via defect species which are usually not present in significant concentration at thermal equilibrium. Under irradiation, D_a is also written as D_{rad}.

In this chapter, we will develop the transient and steady-state solutions to the point defect balance equations in different temperature and microstructure regimes within the framework of radiation-enhanced diffusion [1, 2]. The solutions to the equations are used to determine the radiation-enhanced diffusion coefficient. Reaction rate theory is then presented to develop an understanding of how point

© Springer Science+Business Media New York 2017
G.S. Was, *Fundamentals of Radiation Materials Science*,
DOI 10.1007/978-1-4939-3438-6_5

defects interact with the various defect aggregates. Radiation-enhanced diffusion and defect reaction rate theory are essential to understanding the evolution of the irradiated microstructure developed in Chaps. 6–10.

5.1 Point Defect Balance Equations

The development of radiation-induced vacancy and interstitial concentrations occurs due to competing processes. Frenkel defects are created from the collisions between high-energy particles and lattice atoms. These defects can be lost either through recombination of vacancies and interstitials or by reaction with a defect sink (void, dislocation, dislocation loop, grain boundary, or precipitate). The local change in defect concentration of the various defect species can be written as the net result of (1) the local production rate, (2) reaction with other species, and (3) diffusion into or out of the local volume or the divergence of the flow. The main reactions we will focus on in this treatment are vacancy–interstitial recombination (v + i → □, where □ represents a lattice site) and point defect reactions with sinks (v + s → s, and i + s → s). These competing processes can be mathematically described by the *chemical rate equations*:

$$\begin{aligned}\frac{\mathrm{d}C_\mathrm{v}}{\mathrm{d}t} &= K_0 - K_\mathrm{iv}C_\mathrm{i}C_\mathrm{v} - K_\mathrm{vs}C_\mathrm{v}C_\mathrm{s} \\ \frac{\mathrm{d}C_\mathrm{i}}{\mathrm{d}t} &= K_0 - K_\mathrm{iv}C_\mathrm{i}C_\mathrm{v} - K_\mathrm{is}C_\mathrm{i}C_\mathrm{s},\end{aligned} \tag{5.1}$$

where

C_v vacancy concentration
C_i interstitial concentration
K_0 defect production rate
K_iv vacancy–interstitial recombination rate coefficient
K_vs vacancy–sink reaction rate coefficient
K_is interstitial–sink reaction rate coefficient

The terms K_iv, K_vs, and K_is are the rate constants of the general form, $K_\mathrm{jX,}$ that describe the loss rate of point defects, j per unit point defect concentration to sinks of type, X. Similar equations can be written for defect agglomerates such as di- and trivacancies and interstitials. Note that the equations are nonlinear differential equations and they are not mutually symmetric with respect to vacancy and interstitial concentrations because of the difference in K_is and K_vs, making an analytical solution difficult. The term "chemical" refers to homogeneous reactions, where the rate depends only on concentration ("law of mass action") and not on the local distribution $C(r)$ of the reactants. Thus, uniformity and thereby chemical kinetics require that $\nabla C \approx 0$. This gives rise to a problem when considering localized sinks, e.g., dislocations, grain boundaries, voids, and precipitate interfaces. Such local sinks violate the supposition of spatial uniformity in the host metal

in that there is now locally a directed net flow of mobile point defects toward the closest sinks. The divergence of the flow is equivalent to another "reaction" term, $\nabla \cdot D\nabla C$, in the kinetic balance equations. The locally valid rate equations are as follows:

$$\begin{aligned}\frac{\partial C_\mathrm{v}}{\partial t} &= K_0 - K_\mathrm{iv} C_\mathrm{i} C_\mathrm{v} - K_\mathrm{vs} C_\mathrm{v} C_\mathrm{s} + \nabla \cdot D_\mathrm{v} \nabla C_\mathrm{v} \\ \frac{\partial C_\mathrm{i}}{\partial t} &= K_0 - K_\mathrm{iv} C_\mathrm{i} C_\mathrm{v} - K_\mathrm{is} C_\mathrm{i} C_\mathrm{s} + \nabla \cdot D_\mathrm{i} \nabla C_\mathrm{i}.\end{aligned} \tag{5.2}$$

The solution to these equations requires the statement of boundary conditions in addition to the initial local concentrations of the mobile defects (vacancies and interstitials). However, we can assume that $\nabla C \approx 0$ if the mean defect separation is greater than the mean distance between sinks, that is, the sink density is higher than the defect density. This amounts to treating the sink as being uniformly distributed and Eq. (5.1) applies.

We consider the following model for the solution to Eq. (5.1). A pure metal is irradiated to produce only single vacancies and single interstitials in equal numbers with no spatial correlation of the interstitial with its vacancy. The interstitials and vacancies migrate by random walk diffusion, annihilating each other by mutual recombination or at unsaturable fixed sinks. Sinks and defects are distributed homogeneously in the metal. The diffusion coefficient of the metal is given by the sum of terms due to its diffusion by vacancies and interstitials. The model will have the following limitations:

1. The model applies to a pure metal. Binding of defects to atomic species and limitation of defect motion due to binding and correlation effects are neglected, $f = 1$.
2. The sink concentrations and strengths are time independent, or unsaturable.
3. Other than mutual recombination, defect–defect interactions (e.g., the formation of divacancies or di-interstitials) are ignored.
4. Bias factors for diffusion of defects to sinks are set to unity (no preferential absorption of specific point defects at specific sinks).
5. Diffusion terms in and out of a specific volume are not considered.
6. The thermal equilibrium vacancy concentration is neglected.

The rate constants are as follows:

$$K_\mathrm{iv} = 4\pi r_\mathrm{iv}(D_\mathrm{i} + D_\mathrm{v}) \approx 4\pi r_\mathrm{iv} D_\mathrm{i} \tag{5.3}$$

since $D_\mathrm{i} \gg D_\mathrm{v}$,

$$K_\mathrm{is} = 4\pi r_\mathrm{is} D_\mathrm{i} \tag{5.4}$$

$$K_\mathrm{vs} = 4\pi r_\mathrm{vs} D_\mathrm{v}, \tag{5.5}$$

where r_{iv}, $r_{vs,}$ and r_{is} are interaction radii for the reaction between the species given by the subscripts and represent the radii of surfaces such that if crossed by the defect, it is annihilated. The terms D_i and D_v are the interstitial and vacancy diffusion coefficients, respectively. The production term, K_0, is the *effective* point defect production rate in that it refers to the production of only freely migrating defects that can give rise to long-range diffusion (see Chap. 3). The derivations of the terms in Eqs. (5.3), (5.4), and (5.5) will be given in the Sect. 5.3.

Note that since the rate constants can differ by several orders of magnitude, the equations are stiff. That is, the time increment needed to follow interstitial motion is orders of magnitude too small to show any vacancy motion. Therefore, the equations must be solved using numerical techniques for stiff equations. But we can gain insight into the processes by looking at analytical solutions to limiting cases. For example, the defect concentrations initially increase linearly, with $C_v = C_i = K_0 t$. Further development depends on the values of the temperature and sink concentration, C_s. We will develop analytical solutions to Eq. (5.1) for four different regimes (combinations of T and C_s): (1) low T and low C_s, (2) low T and intermediate C_s, (3) low T and high C_s, and (4) high T.

5.1.1 Case 1: Low Temperature, Low Sink Density

The approximate solutions to Eq. (5.1) for low temperature and low sink density are given in Fig. 5.1. Initially, defect concentrations build up according to $\mathrm{d}C/\mathrm{d}t = K_0$ with $C_i \sim C_v$, so $C_i = C_v = C = K_0 t$. Initially, the concentrations are too low for either recombination or sinks to have an effect on the buildup. The buildup of point defects will start to level off when the production rate is compensated by the recombination rate. In the time regime where the production rate is balanced by the recombination rate, we drop the last two terms from Eq. (5.1) and solve for the "quasi-steady-state" concentrations:

$$\frac{\mathrm{d}C}{\mathrm{d}t} = K_0 - K_{iv}C^2 = 0 \quad (C = C_i = C_v), \tag{5.6}$$

with the solution:

$$C = \left(\frac{K_0}{K_{iv}}\right)^{1/2}. \tag{5.7}$$

Equating this concentration with that during the buildup phase:

$$K_0 t = \left(\frac{K_0}{K_{iv}}\right)^{1/2}, \tag{5.8}$$

yields the time at which losses to recombination compensate for the production rate from irradiation:

$$t = \tau_1 = (K_0 K_{iv})^{-1/2}, \tag{5.9}$$

where τ_1 is a time constant or characteristic time for the *onset of mutual recombination*.

Eventually, the interstitials (first) and then the vacancies (later) will begin to find the sinks, and sinks will start to contribute to annihilation. C_i and C_v remain approximately equal until a time τ_2, which is the time constant for the process of interstitials reacting with the sinks. Because $D_i > D_v$, more interstitials are lost to sinks than vacancies, which is described by:

$$\frac{dC_i}{dt} = -K_{is} C_i C_s, \tag{5.10}$$

so the interstitial concentration will decay and the vacancy concentration will rise (since their only sink is interstitials and interstitials are being lost to sinks), yielding:

$$\begin{aligned} C_v(t) &= \left[\frac{K_0 K_{is} C_s t}{K_{iv}}\right]^{1/2} \\ C_i(t) &= \left[\frac{K_0}{K_{iv} K_{is} C_s t}\right]^{1/2}. \end{aligned} \tag{5.11}$$

(The derivation of Eq. (5.11) is Problem 5.15 at the end of the chapter.) The time at which these equalities occur is obtained by equating the concentrations in the bounding time regimes of quasi-steady state and buildup of interstitials/decay of vacancies (Fig. 5.1):

$$\begin{aligned} C_v &= \left(\frac{K_0}{K_{iv}}\right)^{1/2} = \left[\frac{K_0 K_{is} C_s t}{K_{iv}}\right]^{1/2} \\ C_i &= \left(\frac{K_0}{K_{iv}}\right)^{1/2} = \left[\frac{K_0}{K_{iv} K_{is} C_s t}\right]^{1/2}, \end{aligned} \tag{5.12}$$

and solving for the time yields the time constant for the *onset of the buildup regime*:

$$t = \tau_2 = (K_{is} C_s)^{-1}. \tag{5.13}$$

After a while, at time τ_3, true steady state will be achieved. τ_3 is the time constant for the slowest process, which is the interaction of vacancies with sinks. Solving

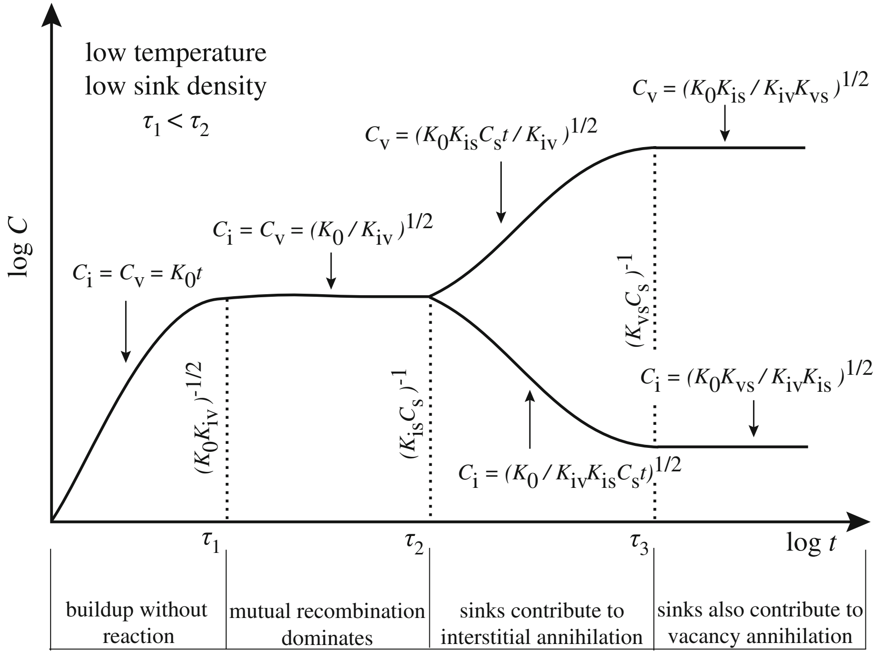

Fig. 5.1 Log–log plot of vacancy and interstitial concentration versus time for case (1) low temperature and low sink density (after [2])

Eq. (5.1) for the steady-state concentration of vacancies and interstitials by setting $dC_v/dt = dC_i/dt = 0$ gives:

$$\begin{aligned} C_v^{ss} &= -\frac{K_{is}C_s}{2K_{iv}} + \left[\frac{K_0K_{is}}{K_{iv}K_{vs}} + \frac{K_{is}^2C_s^2}{4K_{iv}^2}\right]^{1/2} \\ C_i^{ss} &= -\frac{K_{vs}C_s}{2K_{iv}} + \left[\frac{K_0K_{vs}}{K_{iv}K_{is}} + \frac{K_{vs}^2C_s^2}{4K_{iv}^2}\right]^{1/2}. \end{aligned} \tag{5.14}$$

Since vacancies and interstitials are produced in equal numbers and equal numbers are lost to recombination, the loss of each to sinks must be equal at steady state, and:

$$K_{vs}C_v = K_{is}C_i. \tag{5.15}$$

For the case of low temperature and low sink density, C_s is small, and the vacancy and interstitial concentrations in Eq. (5.14) are approximated as:

$$C_v^{ss} \cong \sqrt{\frac{K_0 K_{is}}{K_{iv} K_{vs}}}; \quad C_i^{ss} \cong \sqrt{\frac{K_0 K_{vs}}{K_{iv} K_{is}}}. \tag{5.16}$$

Equating these expressions to those from the previous (buildup) region gives:

$$C_v = \left[\frac{K_0 K_{is} C_s t}{K_{iv}}\right]^{1/2} = \left[\frac{K_0 K_{is}}{K_{iv} K_{vs}}\right]^{1/2}. \tag{5.17}$$

and solving for the time gives the time constant for the *onset of steady state*:

$$t = \tau_3 = (K_{vs} C_s)^{-1}. \tag{5.18}$$

The buildup shown in Fig. 5.1 is really a schematic and not the actual buildup. The transitions between regimes are not so sudden. For example, if the sink density is assumed to be zero, the exact solution to Eq. (5.1) is as follows:

$$C_v(t) = \sqrt{\frac{K_0}{K_{iv}}} \tanh\left(\sqrt{K_{iv} K_0 t}\right). \tag{5.19}$$

5.1.2 Case 2: Low Temperature, Intermediate Sink Density

Increasing the sink density has the effect of bringing τ_2 closer to τ_1 (see Fig. 5.2). That is, the region of mutual recombination is shrunk at the expense of annihilation at sinks. In fact, when:

$$\tau_1 = \tau_2 \text{ or } (K_0 K_{iv})^{-1/2} = (K_{is} C_s)^{-1}, \tag{5.20}$$

the plateau disappears.

5.1.3 Case 3: Low Temperature, High Sink Density

The main effect of a high sink density is that interstitials find the sinks before they find vacancies because $C_s \gg C_v$ at short time (Fig. 5.3). That is, the time to reach linear buildup (loss of interstitials to sinks), τ_2, becomes shorter than the time to reach quasi-steady state due to vacancy–interstitial interaction, τ_1. In this case, the

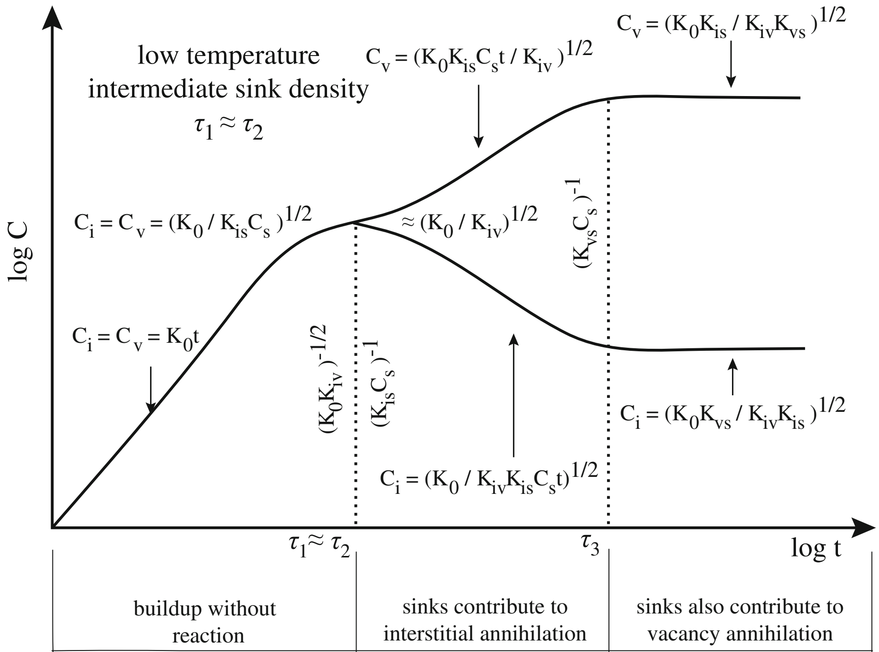

Fig. 5.2 Log–log plot of vacancy and interstitial concentration versus time for case (2) low temperature and intermediate sink density (after [2])

interstitial concentration comes into a quasi-steady state with production and annihilation at sinks:

$$\frac{\mathrm{d}C_i}{\mathrm{d}t} = 0 = K_0 - K_{\mathrm{is}} C_{\mathrm{i}} C_{\mathrm{s}}; \tag{5.21}$$

resulting in the quasi-steady-state concentration:

$$C_{\mathrm{i}} = \frac{K_0}{K_{\mathrm{is}} C_{\mathrm{s}}}. \tag{5.22}$$

Equating interstitial concentrations in the linear buildup regime with the quasi-steady-state regime gives the following:

$$K_0 t = \frac{K_0}{K_{\mathrm{is}} C_{\mathrm{s}}}, \tag{5.23}$$

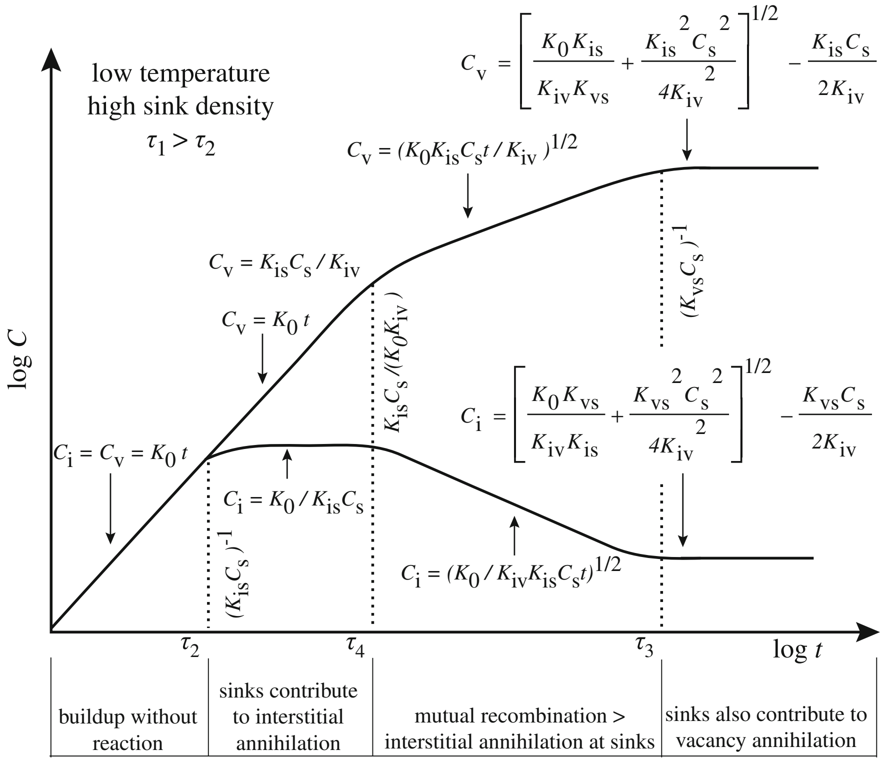

Fig. 5.3 Log–log plot of vacancy and interstitial concentration versus time for case (3) low temperature and high sink density (after [2])

and solving for t gives the value for the time constant τ_2:

$$t = \tau_2 = \left(K_{\rm is}C_{\rm s}\right)^{-1}. \tag{5.24}$$

Note that since interstitials have found the sinks before finding the slower vacancies, the vacancy concentration continues to rise according to $C_{\rm v} = K_0 t$. A competition soon arises between annihilation of interstitials at sinks and recombination with vacancies:

$$K_{\rm is}C_{\rm i}C_{\rm s} = K_{\rm iv}C_{\rm i}C_{\rm v} \cong K_{\rm iv}C_{\rm i}K_0 t, \tag{5.25}$$

yielding the time constant for the transition between the regimes where interstitials go to sinks and mutual recombination dominates:

$$t = \tau_4 = \frac{K_{\rm is}C_{\rm s}}{K_{\rm iv}K_0}. \tag{5.26}$$

In the regime following τ_4, C_v rises but more slowly, and C_i decreases slowly according to:

$$\begin{aligned} C_v &= (K_0 K_{is} C_s t / K_{iv})^{1/2} \\ C_i &= (K_0 / K_{is} K_{iv} C_s t)^{1/2}. \end{aligned} \quad (5.27)$$

Steady state arrives at:

$$\tau_3 = \frac{1}{K_{vs} C_s}, \quad (5.28)$$

with

$$\begin{aligned} C_v^{ss} &= -\frac{K_{is} C_s}{2K_{iv}} + \left[\frac{K_0 K_{is}}{K_{iv} K_{vs}} + \frac{K_{is}^2 C_s^2}{4K_{iv}^2}\right]^{1/2} \\ C_v^{ss} &= -\frac{K_{vs} C_s}{2K_{iv}} + \left[\frac{K_0 K_{vs}}{K_{iv} K_{is}} + \frac{K_{vs}^2 C_s^2}{4K_{iv}^2}\right]^{1/2}. \end{aligned} \quad (5.29)$$

Note that the steady-state concentrations are the same as Eq. (5.14) given earlier in case (1), but without the simplification of dropping the terms in C_s since in this case, the sink density is high and cannot be neglected.

5.1.4 *Case 4: High Temperature*

At high temperature, the defect annihilation rate at the sinks keeps the concentration of interstitials low (Fig. 5.4). Since recombination does not contribute much, the rate equations become the following:

$$\begin{aligned} \frac{dC_v}{dt} &= K_0 - K_{vs} C_s C_v \\ \frac{dC_i}{dt} &= K_0 - K_{is} C_s C_i, \end{aligned} \quad (5.30)$$

with steady-state solutions:

$$C_v = \frac{K_0}{K_{vs} C_s}, \quad C_i = \frac{K_0}{K_{is} C_s}, \quad (5.31)$$

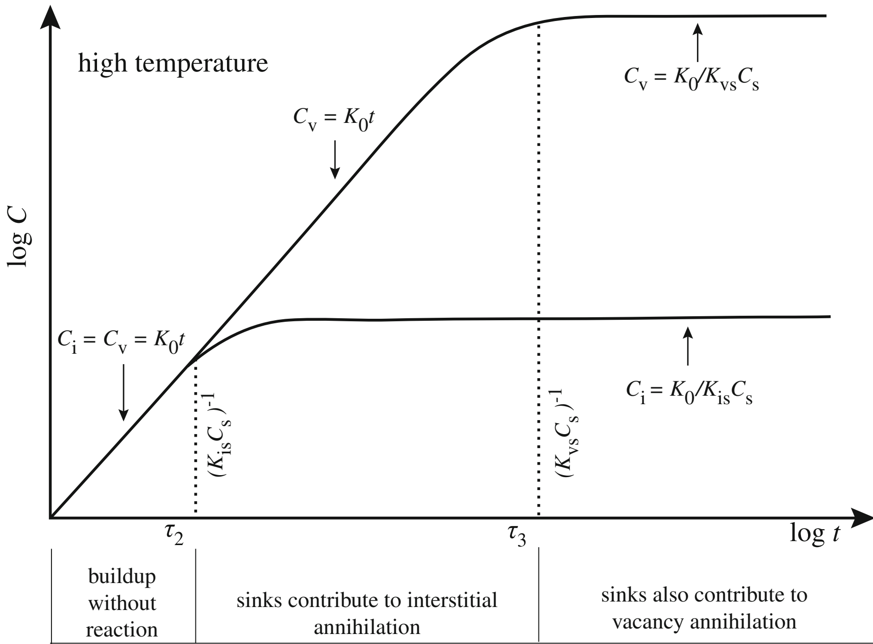

Fig. 5.4 Log–log plot of vacancy and interstitial concentration versus time for case (4) high temperature (after [2])

with characteristic times given by:

$$\text{interstitial annihilation at sinks:}\, K_0 t = \frac{K_0}{K_{is}C_s} \Rightarrow t = \tau_2 = (K_{is}C_s)^{-1} \tag{5.32}$$

$$\text{vacancy annihilation at sinks:}\, K_0 t = \frac{K_0}{K_{vs}C_s} \Rightarrow t = \tau_3 = (K_{vs}C_s)^{-1}. \tag{5.33}$$

The time evolution of vacancy and interstitial concentrations displayed in Fig. 5.4 ignores the presence of thermal vacancies, which may be significant at higher temperatures. The buildup of radiation-induced vacancies and interstitials at high temperature, including an initial presence of thermal equilibrium vacancies, is shown in Fig. 5.5. Note the effect of sink (dislocation) density and defect production rate.

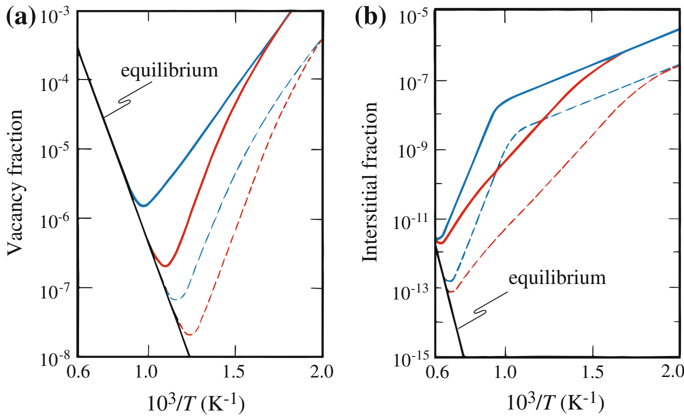

Fig. 5.5 Steady state (**a**) vacancy and (**b**) interstitial concentrations in an irradiated metal at a high production rate (*solid line*) and at a low defect production rate (*dashed line*). The upper (*blue*) and lower (*red*) curves for each defect production rate represent small and large dislocation densities, respectively (after [3])

Figure 5.5a shows that increasing the sink density lowers the vacancy concentration since sinks absorb the vacancies (loss term is proportional to K_{vs}). Also for a fixed sink density, a higher displacement rate results in a higher vacancy concentration because the production rate is higher than the loss rate to sinks. The same is true for interstitials shown in Fig. 5.5b. The kinks in the interstitial concentration curves correspond to the temperature at which vacancies become mobile and contribute to interstitial loss by mutual recombination as in Fig. 5.3. Comparing Fig. 5.5a and b shows that the equilibrium concentration of interstitials is negligible over the practical range of reactor component temperatures, while this is not the case for vacancies.

The main objective of solving the point defect balance equations is to obtain values for C_i and C_v to determine D_{rad}, which is just the sum of C_iD_i and C_vD_v. The preceding discussion shows that we can interpret radiation-enhanced diffusion experiments after an isothermal irradiation at a constant flux for a time t in terms of characteristic times. Table 5.1 summarizes the time constants for the various

Table 5.1 Time constants for rate-limiting processes in the point defect balance equations

Time constant	Value	Process
τ_1	$(K_0 K_{iv})^{-1/2}$	Onset of mutual recombination
τ_2	$(K_{is} C_s)^{-1}$	Onset of interstitial loss to sinks
τ_3	$(K_{vs} C_s)^{-1}$	Onset of vacancy loss to sinks
τ_4	$\tau_1^2/\tau_2 = \frac{K_{is} C_s}{K_0 K_{iv}}$	Mutual recombination dominates interstitial loss to sinks

rate-limiting mechanisms. For low sink density, recombination dominates at short times, followed by interstitial annihilation at sinks and then vacancy annihilation at sinks, which is the slowest process and controls the achievement of steady state. At high sink density, interstitial annihilation at sinks dominates early, followed by mutual recombination and then vacancy loss to sinks. As a rule, when $\tau_1 < \tau_2$, mutual recombination dominates and when $\tau_2 < \tau_1$, sinks dominate. In summary, the key factors affecting C_i and C_v are production rate, defect mobility, and sink concentration.

5.1.5 Properties of the Point Defect Balance Equations

The point defect balance equations and their solutions possess interesting properties, which provide further insight into the behavior of vacancies and interstitials in the diffusion of lattice atoms. They are the following:

1. The vacancy concentration referred to in the last section is really $C_v - C_v^0$ where C_v^0 is the thermal equilibrium concentration of vacancies. In high-temperature irradiations ($T/T_m \geq 0.5$), this concentration is non-negligible. However, over all irradiation temperatures of interest, $C_i^0/C_i \leq 1$.
2. In the absence of sinks and thermal vacancies, C_v can be exchanged with C_i; that is, $C_v = C_i$ at any instant:

$$\begin{aligned} \frac{dC_v}{dt} &= K_0 - K_{iv}C_iC_v \\ \frac{dC_i}{dt} &= K_0 - K_{iv}C_iC_v \end{aligned} \tag{5.34}$$

   Since $D_{rad} = D_iC_i + D_vC_v$, and $C_i = C_v$, but since $D_i \gg D_v$, then interstitials contribute much more to atom mobility than do vacancies.
3. If there is only one type of sink, then at steady state:

$$\begin{aligned} K_0 &= K_{iv}C_iC_v + K_{vs}C_vC_s \\ K_0 &= K_{iv}C_iC_v + K_{is}C_iC_s, \end{aligned} \tag{5.35}$$

   or

$$K_{vs}C_v = K_{is}C_i, \tag{5.36}$$

   and the absorption rate of interstitials and vacancies at sinks is equal, or the net absorption rate at the sink is zero. Even for the case of multiple sink types, if the sinks have the same “strength” for vacancies and interstitials, then the net flow to any sink is zero.

4. Inclusion of sink terms violates the symmetry with respect to C_i and C_v because of the different values of $K(K_{vs} \neq K_{is})$. Symmetry *is* present in the steady state with regard to D_iC_i and D_vC_v (since $K_{is} \propto D_i$ and $K_{vs} \propto D_v$). The consequence is that vacancies and interstitials contribute to atom mobility to the same extent and their actions cannot be discriminated. At steady state:

$$\begin{aligned} 0 &= K_0 - K_{iv}C_iC_v - K'_{vs}D_vC_vC_s \\ 0 &= K_0 - K_{iv}C_iC_v - K'_{is}D_iC_iC_s, \end{aligned} \tag{5.37}$$

where the K terms have been written as $K = K'D$, giving:

$$D_vC_vK'_{vs}C_s = D_iC_iK'_{is}C_s. \tag{5.38}$$

So if $K'_{vs} \sim K'_{is}$, then $D_iC_i = D_vC_v$ which means that vacancies and interstitials contribute *equally* to atom mobility. Even though the steady-state concentration of interstitials is much lower than the steady-state concentration of vacancies, they each contribute equally to atom mobility because of the faster rate of diffusion of interstitials. For any particular sink to grow, it must have a net bias for either vacancies or interstitials. In real metals, K_{vs} and K_{is} are not equal. Specific sinks have a bias for certain point defects, allowing that sink to grow. This behavior is described in more detail in Sect. 5.3.

5.1.6 Deficiencies of the Simple Point Defect Balance Model

The simple point defect model neglects numerous features of realistic systems that must be incorporated in order to obtain accurate results. For example, no account is taken for changing sink strengths, which occur as dose buildup continues due to the formation of depleted zones and defect clusters. Also, sink bias is neglected. Bias is an important factor affecting the development of the irradiated microstructure as will become evident in Chaps. 7 and 8. Defect–defect interaction and defect–impurity interaction have also been neglected. Defect–defect interaction will be important in the formation of void and interstitial loop nuclei and cannot be neglected if larger clusters are to be properly accounted for. These small clusters will serve as traps or sinks for mobile defects. In fact, vacancy clusters have been found to increase D_{rad} in the mutual recombination range, but are insignificant for high sink concentrations and temperatures where annealing to fixed sinks dominates [4]. Finally, the equations are unable to account for defect gradients (and in the simple form, for concentration gradients). These become very important in processes such as radiation-induced segregation (Chap. 6), in which defect fluxes give rise to concentration gradients in the alloying elements. Such processes may significantly alter the behavior of sinks and the bias of the sinks.

5.1.7 *Point Defect Balance Equations in the Presence of Cascades*

In a cascade, vacancies and interstitials are produced simultaneously but in a segregated fashion such that their distributions are separated from each other in space [5]. After the initial thermal annealing period, vacancies segregate in a vacancy-rich region (e.g., Figs. 3.3 and 3.4). Because of their high concentration and high mobility, the interstitials immediately start to form clusters [6] and diffuse at the same time. In molecular dynamics simulation of cascades, the interstitials are consistently observed to form clusters even in low energy (≈1–2 keV) cascades. More interstitial clustering is likely to occur in higher energy cascades since the concentration of interstitials in these cascades is likely to be higher. These clusters have been found to be stable even at high temperatures. In general, the interstitial population is likely to be partitioned into three portions: one that back diffuses into the vacancy-rich zone and is lost through recombination with the vacancies, one that is immobilized through interaction and clustering, and one that escapes the cascade zone and engages in long-range migration. The relative proportion of these three portions may be affected by the size and morphology of cascades and the disposition of sinks in the vicinity of the cascade.

The vacancy population in the cascade core agglomerates during the "cool down" period after the collision event and eventually collapses to form vacancy loops or stacking fault tetrahedra. In the temperature range of interest, the immobilization of vacancies in vacancy loops is only temporary. They will soon be re-emitted during thermal annealing and become available to various sinks, including voids, as freely migrating vacancies. At elevated temperatures (e.g., the peak swelling temperature), vacancy loops are thermally unstable because of the high line tension and would shrink by vacancy emission. The evaporation of vacancies from the loops and their escape from the vacancy-rich zone provides the mobile vacancies for microstructural evolution (e.g., void growth) and macroscopic deformation.

On the other hand, the immobilization of interstitials in the interstitial loops is permanent. Due to their high formation energy, they remain locked in interstitial loops from the moment they are created. They are unavailable to the voids, whether they grow to a network by receiving a net flow of interstitials, or shrink out of existence by absorbing a net flow of vacancies, or are destroyed by dislocation sweep or cascade overlap. The lifetime of vacancy loops is dominated by thermal annealing and that of the interstitial loops is dominated by destruction.

This description of vacancies and interstitials in the cascade process means that there is an *asymmetry* in the production of mobile point defects (that enters into the mean-field description of microstructure evolution followed by the rate theory approach). First, the proportion of vacancies that agglomerate into clusters is not likely to be the same as that of the interstitials. Second, even if they are, while the vacancy loops can still provide mobile vacancies by evaporation, the interstitial clusters cannot. Thus, it is the difference in the stability and lifetime between

vacancy and interstitial clusters generated during the cascade process that gives rise to a biased production of available vacancies and interstitials. This *production bias* could be a potent driving force for void growth and swelling during cascade damage conditions.

It should be noted that the concept of production bias is valid not only for low doses but also for high doses. One process that could maintain operation of the production bias even at high doses is the climb or/and glide of dislocation segments during irradiation. The mobile dislocation segments would keep sweeping the interstitial clusters and would prevent the buildup of a high concentration of interstitials in the form of clusters. However, bias is absent in the case of electron irradiation when only Frenkel pairs are produced.

In case of cascade production, Eq. (5.1) must be modified to incorporate the effect of production bias. If ε_r is the fraction of defects that recombine in the cascade and ε_v and ε_i are the fractions of clustered vacancies and interstitials, respectively, then the production of isolated vacancies and interstitials is given as:

$$\begin{aligned} K_v &= K_0(1-\varepsilon_r)(1-\varepsilon_v) \\ K_i &= K_0(1-\varepsilon_r)(1-\varepsilon_i), \end{aligned} \tag{5.39}$$

and the point defect balance equations become the following:

$$\begin{aligned} \frac{dC_v}{dt} &= K_0(1-\varepsilon_r)(1-\varepsilon_v) - K_{iv}D_vC_v - K_{vs}C_vC_s + L_v \\ \frac{dC_i}{dt} &= K_0(1-\varepsilon_r)(1-\varepsilon_i) - K_{iv}D_vC_v - K_{is}C_iC_s, \end{aligned} \tag{5.40}$$

where L_v is the production of thermal vacancies from the various sinks (discussed in more detail in Sect. 8.2.1). The continuous production of single interstitial atom (SIA) clusters in displacement cascades is a key process that makes microstructure evolution under cascade conditions qualitatively different from that during Frenkel pair (FP) producing electron irradiation. For electron irradiation, Eq. (5.1) describes the evolution of the defect concentration. In the case of production of clusters in irradiations that generate cascades, Eq. (5.40) should be used.

However, another factor that impacts isolated defect concentration is the mobility of SIA clusters. These clusters have been found to exhibit one-dimensional (1D) migration rather than 3D migration characteristic of isolated point defects. This high mobility results in the constant removal of SIA clusters from the bulk, further increasing the defect imbalance. Note that SIA cluster removal by 1D migration means that dislocation sweeping of clusters is not required to prevent the buildup of the interstitial cluster concentration at high dose.

Damage accumulation under cascade conditions requires the inclusion of the mobile (glissile) SIA cluster concentration, $C_{giL}(x)$, in the defect balance equations of Eq. (5.40):

$$\begin{aligned}
\frac{\mathrm{d}C_{\mathrm{v}}}{\mathrm{d}t} &= K_0(1-\varepsilon_{\mathrm{r}})(1-\varepsilon_{\mathrm{v}}) - K_{\mathrm{iv}}D_{\mathrm{v}}C_{\mathrm{v}} - K_{\mathrm{vs}}C_{\mathrm{v}}C_{\mathrm{s}} + L_{\mathrm{v}} \\
\frac{\mathrm{d}C_{\mathrm{i}}}{\mathrm{d}t} &= K_0(1-\varepsilon_{\mathrm{r}})(1-\varepsilon_{\mathrm{i}}) - K_{\mathrm{iv}}D_{\mathrm{v}}C_{\mathrm{v}} - K_{\mathrm{is}}C_{\mathrm{i}}C_{\mathrm{s}} \\
\frac{\mathrm{d}C_{\mathrm{giL}}(x)}{\mathrm{d}t} &= K_{\mathrm{giL}}(x) - K_{\mathrm{g}}(x)C_{\mathrm{i}}C_{\mathrm{giL}}(x),
\end{aligned} \tag{5.41}$$

where $C_{\mathrm{giL}}(x)$ is the concentration, $K_{\mathrm{giL}}(x)$ is the production rate, and $K_{\mathrm{g}}(x)$ is the rate constant for interstitial interaction with glissile SIA loops (clusters) of size x. The solution of Eq. (5.41) will be discussed in Chap. 8, Sect. 8.3.8 on void swelling.

5.2 Radiation-Enhanced Diffusion

In a pure metal, the diffusion coefficient under radiation is given by:

$$D_{\mathrm{rad}} = D_{\mathrm{v}}C_{\mathrm{v}} + D_{\mathrm{i}}C_{\mathrm{i}}. \tag{5.42}$$

Because the concentrations of vacancies and interstitials under irradiation are much greater than those produced thermally, the radiation-enhanced diffusion coefficients are much larger than thermal diffusion coefficients. Despite the shortcomings, it is interesting to see how well the simple point defect balance equations are able to estimate the effect of irradiation on diffusion. Figure 5.6 shows a plot of log D_{rad}

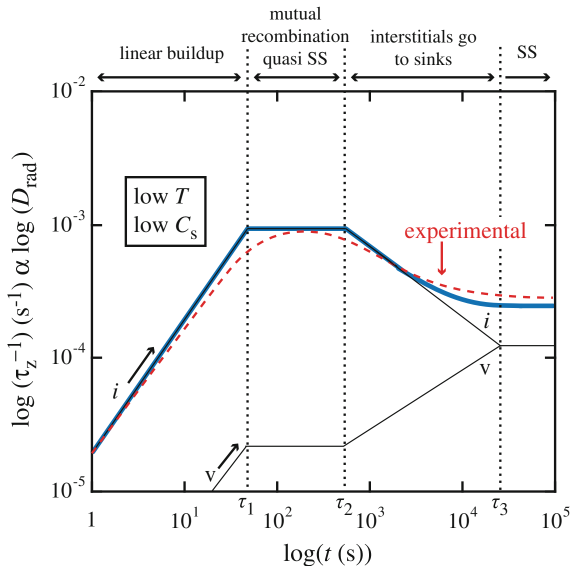

Fig. 5.6 Time dependence of log(D_{rad}) versus log(t) for both calculation (*solid line*) and measurement (*dashed red line*). *Thin solid black lines* are for the vacancy and interstitial components and the *heavy solid blue line* is the sum of the components (after [2])

versus log t for the case of annealed Ag-30 % Zn at 40 °C irradiated with 2.5 MeV electrons at a flux of 3.7×10^{15} m^{-2} s^{-1} [2]. The thin solid black lines are the interstitial and vacancy components and the thick solid blue line is their sum as calculated from Eq. (5.42) by Sizeman [2], and the dashed red line is the experimental data. The experiment actually measures the Zener relaxation time, τ_z (see [1]), which is proportional to D_{rad}. The experimental result confirms the existence of a maximum in D_{rad} as in case (1) for low temperature and low sink density. This result also shows that the interstitial component dominates at times less than that to achieve steady state, τ_3, since $D_i > D_v$ (by assumption) and $C_i > C_v$ for $\tau < \tau_3$.

Another excellent example of calculation of D_{rad} verses measurement is provided by Rothman [1] for self-diffusion in copper at 200 °C in a crystal containing a dislocation density of 10^{11} m^{-2} under irradiation with a net damage rate, $K_0 = 10^{-6}$ dpa/s (similar to that experienced by a fast reactor core structural material). In this case, $D_{rad} \sim 6.5 \times 10^{-21}$ m^2 s^{-1}. Given that the thermal diffusion coefficient is $\sim 1.4 \times 10^{-27}$ m^2 s^{-1}, this represents an extremely large ($>10^6$) increase due to irradiation. Figure 5.7 shows that at temperatures below 575 °C, D_{rad} exceeds the thermal equilibrium self-diffusion coefficient for this defect production rate (curve 1). The various curves in Fig. 5.7 represent different combinations of production rates and defect densities. Note that at low temperature, mutual recombination dominates and D_{rad} has an activation energy of $E_m^v/2$ (all curves). At low sink density (10^{11} dislocations m^{-2} (curve 1), where $\rho_d \sim 4\pi r_{vs}C_s = 4\pi r_{is}C_s$), the mutual recombination region ties indirectly to diffusion by

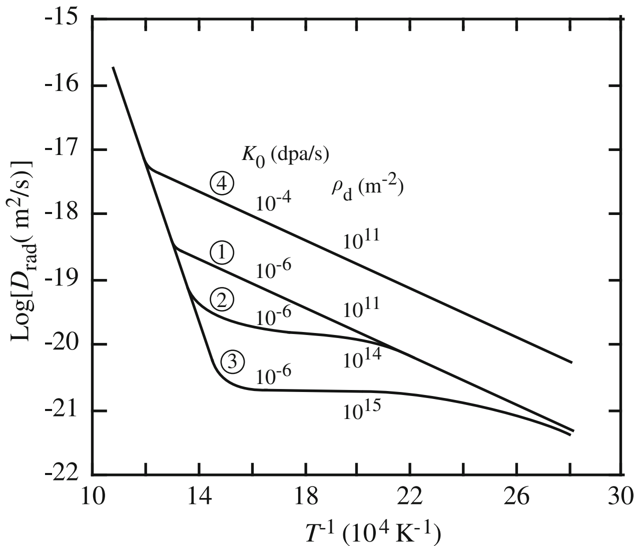

Fig. 5.7 Calculated D_{rad} for self-diffusion of copper as a function of temperature for different combinations of defect production rates and dislocation densities. (1) $K_0 = 10^{-6}$ dpa/s, $\rho_d = 10^{11}$ m^{-2}, (2) $K_0 = 10^{-6}$ dpa/s, $\rho_d = 10^{14}$ m^{-2}, (3) $K_0 = 10^{-6}$ dpa/s, $\rho_d = 10^{15}$ m^{-2}, (4) $K_0 = 10^{-4}$ dpa/s, $\rho_d = 10^{11}$ m^{-2} (after [1])

thermal equilibrium vacancies with increasing temperature. At high sink densities, [10^{14} m^{-2} (curve 2) and 10^{15} m^{-2} (curve 3)], mutual recombination gives way to annealing at fixed sinks at a critical temperature, determined as follows.

According to Eq. (5.36), for a single sink type:

$$C_i K_{is} = C_v K_{vs} \quad \text{or} \quad C_i = \frac{C_v K_{vs}}{K_{is}}. \tag{5.43}$$

At steady state, Eq. (5.29) is applied and they can be rewritten in the following form:

$$\begin{aligned} C_v &= \frac{K_{is} C_s}{2K_{iv}} \left[\left(1 + \frac{4K_0 K_{iv}}{K_{is} K_{vs} C_s^2} \right)^{1/2} - 1 \right] \\ C_i &= \frac{K_{vs} C_s}{2K_{iv}} \left[\left(1 + \frac{4K_0 K_{iv}}{K_{is} K_{vs} C_s^2} \right)^{1/2} - 1 \right]. \end{aligned} \tag{5.44}$$

We define a parameter, η, such that:

$$\eta = \frac{4K_0 K_{iv}}{K_{vs} K_{is} C_s^2}. \tag{5.45}$$

Then using Eq. (5.44), C_v can be written as:

$$C_v = \frac{F(\eta) K_0}{K_{vs} C_s}, \quad \text{or} \quad C_v K_{vs} C_s = F(\eta) K_0. \tag{5.46}$$

where

$$F(\eta) = \frac{2}{\eta}[1 + \eta)^{1/2} - 1]. \tag{5.47}$$

Equation (5.46) shows that $F(\eta)$ determines the number of defects absorbed by sinks in relation to the total rate of formation of the defects. If $\eta \rightarrow 0$, then $F(\eta) \rightarrow 1$, i.e., all of the defects are lost to sinks and none to recombination. In the limit of large η, $F(\eta) \sim 2/\eta^{1/2}$ and $F(\eta) \rightarrow 0$, indicating that mutual recombination dominates defect loss. When $F(\eta) = 1/2$, the loss of defects to sinks and recombination is equal. This occurs at a value of η of:

$$\eta = 8 = \frac{4K_0 K_{iv}}{K_{vs} K_{is} C_s^2}. \tag{5.48}$$

Equation (5.48) can be solved for the critical temperature below which mutual recombination will dominate, and above which loss to sinks will dominate. (The term η will be revisited in Chap. 8 in describing the effect of recombination on

void growth). Using Eqs. (5.3), (5.4), and (5.5) for K_{iv}, K_{is}, and K_{vs}, and defining $K'_{iv} = 4\pi r_{iv}, K'_{is} = 4\pi r_{is}$, and $K'_{vs} = 4\pi r_{vs}$, Eq. (5.48) can be written as:

$$8 = \frac{4K_0 K'_{iv} D_0^i \exp\left(\frac{-E_m^i}{kT}\right)}{K'_{vs} D_0^v \exp\left(\frac{-E_m^v}{kT}\right) K'_{is} D_0^i \exp\left(\frac{-E_m^i}{kT}\right) C_s^2}, \tag{5.49}$$

where $E^v_{i,m}$ is the migration energy and $D_0^{i,v}$ is the pre-exponential factor in the diffusion coefficient for interstitials and vacancies, respectively. Equation (5.49) simplifies to:

$$T_c = \frac{E_m^v}{k \ln\left[\frac{2D_0^v C_s^2 K'_{is} K'_{vs}}{K_0 K'_{iv}}\right]}. \tag{5.50}$$

At the highest temperatures, D_{rad} is overwhelmed by thermal vacancies (all curves in Fig. 5.7), and increasing K_0 to 10^{-4} dpa/s (curve 4) raises D_{rad} in the mutual recombination range by a factor of 10.

Figure 5.8 shows the radiation-enhanced diffusion coefficient calculated for a sample of nickel undergoing irradiation at a rate of 10^{-6} dpa/s for different sink annihilation probabilities, p, where p^{-1} is the average number of jumps of a defect between creation and annihilation at a sink [7]. The diffusion coefficient describing radiation-enhanced diffusion, D_{rad}, is shown by the solid line. The dashed line to the left is the thermal diffusion coefficient and the solid horizontal line at the right is the diffusion coefficient due to ballistic mixing, D_m [8], and will be discussed in Chap. 10.

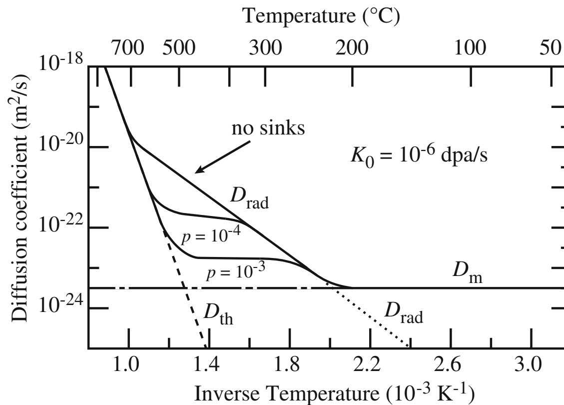

Fig. 5.8 Diffusion coefficient as a function of $1/T$ for a nickel-base alloy during irradiation at a displacement rate of 10^{-6} dpa/s. D_{rad} is calculated from rate theory for various sink annihilation probabilities, p. The diffusion coefficient from displacement mixing is D_m and the thermal diffusion coefficient is D_{th} (after [7])

The difference between the curves for D_{rad} and D_{th} is the effect of radiation-enhanced diffusion. As shown, irradiation can result in a several orders of magnitude increase in the diffusion coefficient.

5.3 Defect Reactions

Each of the terms in the point defect balance equations represents a reaction. The rate at which the reaction occurs will depend on the nature of the reacting species. Following [3], we will develop expressions for the rates of each of the reactions in the point defect balance equations, as they will be used in describing processes such as void growth and dislocation climb. We have seen that the motion of mobile point defects can be considered a random walk process. When one of these defects encounters a specie in the crystal to which it becomes tightly bound, one or both of the partners in the encounter are considered to disappear from the solid. Examples include a vacancy or interstitial intersecting a free surface, grain boundary, dislocation, void, etc., or a vacancy encountering a vacancy, an interstitial encountering an interstitial, or a vacancy encountering an interstitial. Clearly, the rate of such reactions is proportional to the concentrations of both species, or:

$$\text{reaction rate of A and B} = K_{\mathrm{AB}} C_{\mathrm{A}} C_{\mathrm{B}} \ \text{reaction/cm}^3\,\text{s}, \tag{5.51}$$

where C_{A} and C_{B} are the concentrations of species A and B in units of particles/cm^3, and K_{AB} is the rate constant of the reaction in cm^3/s. Reactions can be between two mobile particles (vacancy and interstitial at high temperature) or between one mobile and one stationary defect, e.g., low temperature where vacancies are immobile and interstitials are mobile, or between interstitials and dislocation, grain boundaries, and voids.

There are two types of processes that will be of interest in dealing with the reaction between point defects and sinks; reaction rate-controlled and diffusion-controlled. In reaction rate-governed processes, there must be no macroscopic concentration gradients of either partner. If one partner is large compared to the atomic-sized reactant, or if one is a strong sink, a concentration gradient may be established in the vicinity of the stationary defect. Reactions between point defects are examples of reaction rate-controlled processes. If a defect concentration gradient is established, the overall process is governed by the rate of diffusion of the mobile species to the stationary sink. This is the case with free surfaces, voids, and grain boundaries. These defects are usually not treated by reaction rate theory.

As a first example of a reaction rate-controlled process, let us look at the vacancy–vacancy reaction. Consider the reaction:

$$\mathrm{v} + \mathrm{v} \rightarrow \mathrm{v}_2, \tag{5.52}$$

that proceeds in the forward direction only and is characterized by the rate constant K_{2v}. In this example, one vacancy is assumed to be stationary and the other is mobile. The rate of divacancy formation per cm^3 is given as:

$$R_{2v} = P_{2v}C_v, \tag{5.53}$$

where C_v is the concentration of monovacancies and P_{2v} is the probability per second that another vacancy jumps into a site that is a nearest neighbor to a particular vacancy (Fig. 5.9). A divacancy will form if a nearest neighbor site to a vacancy is occupied by another vacancy, thus P_{2v} depends on the crystal structure. Taking the fcc lattice, all 12 nearest neighbor sites are equivalent, yielding:

$$P_{2v} = 12P_x, \tag{5.54}$$

where P_x is the probability per second that another vacancy jumps into one of the nearest neighbor positions surrounding the vacancy. P_x is proportional to:

1. The number of sites surrounding the nearest neighbor site from which another vacancy could jump (seven sites as shown by the open red circles in Fig. 5.9)
2. The probability that one of these lattice positions is occupied by a vacancy, N_v
3. The jump frequency of a vacancy, ω, or

$$P_x = 7N_v\omega, \tag{5.55}$$

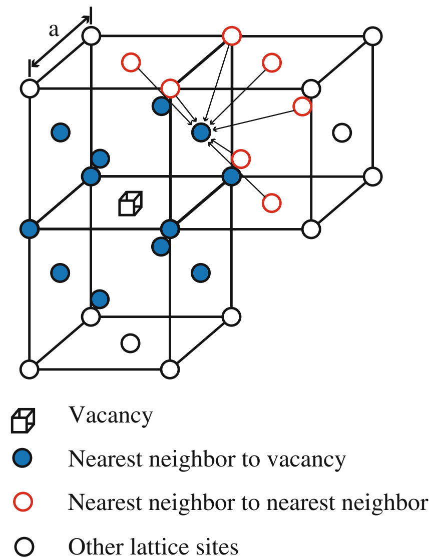

Fig. 5.9 Locations of nearest neighbors for the formation of a divacancy in the fcc lattice (after ref. [3])

and we can write the vacancy site fraction as $N_v = C_v\Omega$, where C_v is the volumetric vacancy concentration and Ω is the atomic volume. Back substitution of Eqs. (5.54) and (5.55) into Eq. (5.53) yields:

$$R_{2v} = 84\omega\Omega C_v^2 [\mathrm{cm}^{-3}\,\mathrm{s}^{-1}]. \tag{5.56}$$

Comparison with the definition of the reaction rate, Eq. (5.51) gives the reaction rate constant K_{2v}:

$$K_{2v} = 84\omega\Omega. \tag{5.57}$$

In the fcc lattice, $D = a^2\omega$, then:

$$K_{2v} = \frac{84\Omega D_v}{a^2}. \tag{5.58}$$

Although the expression for the rate constant was derived for a vacancy–vacancy reaction, the same formulation applies to any reaction between any specie (e.g., impurity) that occupies substitutional positions in the fcc lattice. It can also be used for other lattice types, but the factor, 84, called the combinatorial factor, or z, is dependent on the crystal structure. The combinatorial factor is the solid-state analog of the cross section in particle interactions.

In the previous example, we forced one of the reactants to be stationary. When the reaction is between two mobile species, the rate is $(K_{AB} + K_{BA})\, C_A C_B$, where K_{AB} is the rate constant calculated assuming that B is immobile and vice versa for K_{BA}. Therefore, if both vacancies are mobile, the result would be multiplied by a factor of 2; $K_{2v} + K_{2v} = 2K_{2v}$. Given this background, we now turn our attention to the various terms in the point defect balance equations in order to develop expressions for the reaction rate coefficients.

5.3.1 Defect Production

The first term in the defect balance equations of Eq. (5.1) is the production rate of vacancies and interstitials and this was determined in Chap. 2, Eq. (2.125), where the term in brackets is given the designation, ν_{FP}

$$K_0 = \xi \nu_{FP} \sigma_s N \phi [\mathrm{cm}^{-3}\,\mathrm{s}^{-1}]. \tag{5.59}$$

For stainless steel, $\nu_{FP} \sim 30$ Frenkel pairs per collision, $\sigma_s \sim 3 \times 10^{-24}$ cm^2 and $N \sim 7 \times 10^{22}$ cm^{-3}. The term, ξ, is the displacement efficiency (Chap. 3) that accounts for the reduction in freely migrating point defects due to in-cascade recombination and clustering.

5.3.2 Recombination

The second term in Eq. (5.1), $K_{iv}C_vC_i$, is the recombination rate. The rate constant K_{iv} is the same for both vacancies and interstitials since they must recombine with each other at the same rate. Reactions between vacancies and interstitials are of great importance since the result is mutual annihilation or return to the perfect lattice. Assuming a stationary vacancy and a mobile interstitial, and that recombination occurs only when the interstitial jumps into a site that is nearest neighbor to the vacancy, we can determine the recombination rate constant for an octahedral interstitial in the fcc lattice. There are six octahedral sites as nearest neighbors to the vacant lattice site and each interstitial site has eight octahedral nearest neighbors, giving a value of 48 for the combinatorial factor:

$$K_{iv} = \frac{48\Omega D_i}{a^2}. \tag{5.60}$$

However, this is a bit unrealistic since (1) the stable form of the interstitial is the split interstitial and (2) the vacancy and interstitial are attracted to each other by virtue of their strain fields, causing spontaneous recombination to occur over distances greater than the nearest neighbor spacing. Therefore, a more realistic estimate of the combinatorial factor, z_{iv}, is ~ 500:

$$K_{iv} = \frac{z_{iv}\Omega D_i}{a^2}, \quad \text{and} \quad z_{iv} \sim 500. \tag{5.61}$$

5.3.3 Loss to Sinks

The loss term represents all the possible sinks for vacancy and interstitial loss. These sinks can be divided into three categories:

1. *Neutral* (*unbiased*) *sinks* show no preference for capturing one type of defect over the other type. The rate of absorption is proportional to the product of the diffusion coefficient of the point defect and the difference in the concentrations of the point defect in the bulk metal and at the sink surface. The types of sinks in this category are voids, incoherent precipitates, and grain boundaries.
2. *Biased sinks* exhibit preferential attraction for one defect type over the other. Dislocations exhibit a stronger preference for interstitials than for vacancies. The bias is due to the drift of interstitials down the stress gradient near the dislocation core. Since absorption of interstitials enhances dislocation climb, the dislocation is an unsaturable sink. Two types of dislocations are considered:

networks in unirradiated metal and from unfaulted Frank loops, and interstitial dislocation loops.

3. *Variable bias sinks* such as coherent precipitates act as traps that capture a defect but preserve its identity until it is annihilated by the opposite type defect. Impurity atoms and coherent precipitates act as recombination centers with a limited capacity.

5.3.4 Sink Strengths

Reaction rate constants describe the reaction between a point defect and a sink (which may be another point defect), and are designated K_{jX} where j is the mobile point defect and X is the sink. As such, they include the diffusion coefficient of the point defect as well as a description of the tendency for the reaction to occur. It is often useful to describe the tendency of a sink to absorb defects that is independent of the defect properties. The sink strength, with units of [cm^{-2}], is such a description and it reflects the strength or affinity of a sink for defects. Sink strength is independent of defect properties for neutral sinks. The sink strength is denoted by k^2_{jX}, and is defined as:

$$\text{absorption rate} = K_{jX}C_jC_X = k^2_{jX}C_jD_j, \tag{5.62}$$

so

$$k^2_{jX} = \frac{K_{jX}C_X}{D_j}, \tag{5.63}$$

or

$$k^2_j = \sum_X k^2_{jX}. \tag{5.64}$$

Both the rate constant and the sink strength are terms commonly used to describe the action of sinks on the defects in the solid. Physically, k_j^{-1} is the mean distance a free defect of type j travels in the solid before becoming trapped.

Before we treat the various sink types, we will first look at the rate constants for the two basic reaction processes: reaction rate-controlled processes and diffusion-limited processes. We begin with reaction rate-controlled processes.

5.4 Reaction Rate-Controlled Processes

5.4.1 Defect–Void Interaction

For reactions where capture is controlled by the rate at which the point defects enter the trap site, we can use Eq. (5.61). For defect–void reactions, the term to be determined is the combinatorial factor. For a void, the number of lattice points on the surface of the sphere is $4\pi R^2/a^2$, where the area occupied by a lattice point is approximated by a^2. The rate constant then becomes:

$$K_{\mathrm{vV}} = \frac{4\pi R^2 \Omega D_{\mathrm{v}}}{a^4} = \frac{4\pi R^2 D_{\mathrm{v}}}{a}, \quad \text{where } \Omega \sim a^3, k_{\mathrm{V}}^2 = \frac{4\pi R^2 \rho_{\mathrm{V}}}{a}, \tag{5.65}$$

where ρ_{V} is the concentration of voids in the solid.

5.4.2 Defect–Dislocation Interaction

Consider a cylinder about a dislocation line whose axis is coincident with the dislocation line such that capture is certain for any vacancy entering the cylinder (Fig. 5.10). The cylinder consists of z_{vd} atomic sites on each of the crystal planes intersected by the dislocation line. The cylinder defines the capture radius of the dislocation, or the radius inside which entering defects are lost to the sink. If the spacing between atom planes in the lattice is $\sim a$, then there are z_{vd}/a capture sites per unit length of dislocation. Letting ρ_{d} be the density of dislocation lines in the crystal (in units of centimeters of dislocation line per cm^3 of solid or cm^{-2}), then there are $z_{\mathrm{vd}} \rho_{\mathrm{d}}/a$ capture sites per unit volume. If the concentration of vacancies per unit volume

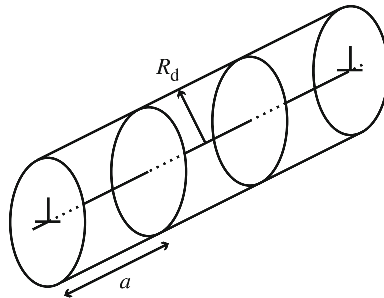

Fig. 5.10 Capture volume around a dislocation line, defined by the cylinder of radius R_{d} and with sink sites lying on crystal planes separated by a distance a

is C_v, then the vacancy site fraction is $C_v\Omega$. For a vacancy jump rate of ω, the rate of vacancy capture rate by the dislocation per cm^3 is given as:

$$R_{vd} = \frac{z_{vd}\rho_d}{a} C_v \Omega \omega \ [\mathrm{cm}^{-3}\,\mathrm{s}^{-1}]. \tag{5.66}$$

Since $\Omega \sim a^3$ and $D_v = a^2\omega$, we have:

$$\begin{aligned} R_{vd} &= D_v z_{vd} \rho_d C_v \text{ and reaction rate constant } K_{vd} = D_v z_{vd}, k^2_{vd} = z_{vd}\rho_d \\ R_{id} &= D_i z_{id} \rho_d C_i \text{ and reaction rate constant } K_{id} = D_i z_{id}, k^2_{id} = z_{id}\rho_d \end{aligned} \tag{5.67}$$

and $z_{vd} \neq z_{id}$.

5.5 Diffusion-Limited Reactions

Reactions between defects and sinks cannot always be characterized as reaction rate-limited. Reactions driven by defect concentration gradients are diffusion-limited and must be treated differently. Such reactions are defect–void, defect–grain boundary, and sometimes defect–dislocation interactions. Following [3], these reactions are addressed here starting with defect–void reactions.

5.5.1 Defect–Void Reactions

Consider the case of ρ_V voids per unit volume, each of radius, R, which absorb a particular type of point defect present in the solid and between the spherical sinks. Focusing on a single sphere, the unit cell or capture volume surrounding each sphere is defined as the portion of the solid that can be associated with each sphere. The radius of the capture volume (see Fig. 5.11) around each sphere is defined by:

$$\left(\frac{4}{3}\pi\mathscr{R}^3\right)\rho_V = 1. \tag{5.68}$$

The diffusion equation for the point defects will be solved in the spherical shell $R \le r \le \mathscr{R}$. The concentration of point defects at a radial position r in the capture volume at time t is denoted by $C(r, t)$. The definition of the capture volume implies that there is no net flux of point defects across the boundary at $r = \mathscr{R}$, which is written as:

$$\left(\frac{\partial C}{\partial r}\right)_{\mathscr{R}} = 0, \tag{5.69}$$

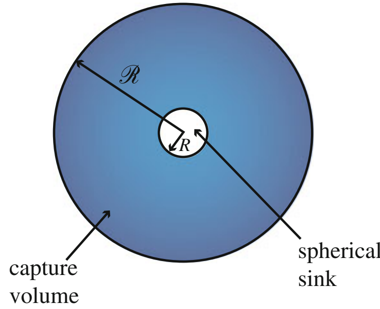

Fig. 5.11 The unit cell for determination of the diffusion-controlled rate constant for defect absorption by a spherical sink

and the point defect concentration at the surface of the sphere is given as:

$$C(R, t) = C_{\mathrm{R}}. \tag{5.70}$$

The value of C_{R} depends on the process. For insoluble gas atoms where the spheres represent gas bubbles, $C_{\mathrm{R}} = 0$. For bubbles or voids where the point defects are vacancies or interstitials, $C_{\mathrm{R}} = C^{0}_{\mathrm{v,i}}$, the thermal equilibrium defect concentration.

If the defects are created uniformly in the capture volume and no sinks other than the sphere are present, then the concentration $C(r, t)$ is determined by solution of the volumetric diffusion equation with a volumetric source term:

$$\frac{\partial C}{\partial t} = \frac{D}{r^2}\frac{\partial}{\partial r}\left(r^2\frac{\partial C}{\mathrm{d}r}\right) + K_0, \tag{5.71}$$

where D is the diffusion coefficient of the defects (assumed to be independent of concentration) and K_0 is the defect production rate per unit volume given by Eq. (5.59).

When a solid is irradiated at a temperature where point defects are mobile, the loss of particles to the sink is partially compensated by the production rate so the concentration changes slowly with time $\left(\frac{\partial C}{\partial t} \sim 0\right)$ and Eq. (5.71) can be approximated as:

$$\frac{D}{r^2}\frac{\mathrm{d}}{\mathrm{d}r}\left(r^2\frac{\mathrm{d}C}{\mathrm{d}r}\right) = -K_0. \tag{5.72}$$

The solution to Eq. (5.72) subject to the boundary conditions given by Eqs. (5.69) and (5.70) is given as:

$$C(r) = C_{\mathrm{R}} + \frac{K_0}{6D}\left[\frac{2\mathscr{R}^2(r-R)}{rR} - (r^2 - R^2)\right]. \tag{5.73}$$

Since in many cases, the capture volume radius is much larger than the sink radius and the defect concentration changes rapidly only very close to the sink, the capture volume is divided into two regions (Fig. 5.12). In region 1, the diffusion term is much greater than the source term and Eq. (5.72) can be approximated by:

$$\frac{1}{r^2}\frac{\mathrm{d}}{\mathrm{d}r}\left(r^2\frac{\mathrm{d}C}{\mathrm{d}r}\right) = 0, \tag{5.74}$$

with boundary conditions:

$$C(R) = C_{\mathrm{R}} \tag{5.75}$$

$$C(\infty) = C(\mathscr{R}). \tag{5.76}$$

The solution of Eq. (5.74) subject to the boundary conditions given by Eqs. (5.75) and (5.76) gives:

$$C(r) = C_{\mathrm{R}} + [C(\mathscr{R}) - C_{\mathrm{R}}]\left[1 - \left(\frac{R}{r}\right)\right]. \tag{5.77}$$

The flux of particles at the void surface is defined by:

$$J = -D\left(\frac{\mathrm{d}C}{\mathrm{d}r}\right)_R. \tag{5.78}$$

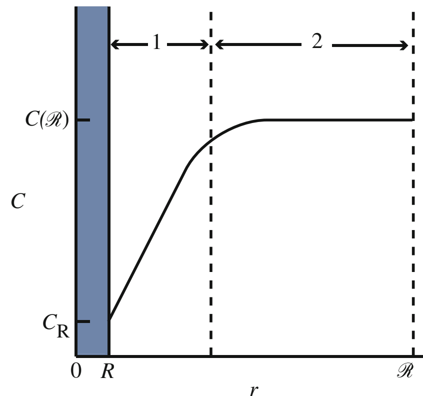

Fig. 5.12 Regions of interest in the solution of the diffusion equation in a spherical shell with a uniform volumetric production rate of defects

Using Eq. (5.77) gives:

$$J = \frac{-D[C(\mathscr{R}) - C_{\mathrm{R}}]}{R}. \tag{5.79}$$

The absorption rate of point defects by the void is given as:

$$-(4\pi R^2)J = 4\pi RD[C(\mathscr{R}) - C_{\mathrm{R}}]. \tag{5.80}$$

Requiring that point defects produced in the capture volume be absorbed by the void gives:

$$\frac{4}{3}\pi\left(\mathscr{R}^3 - R^3\right)K_0 = 4\pi RD[C(\mathscr{R}) - C_{\mathrm{R}}]. \tag{5.81}$$

If $\mathscr{R}^3 \gg R^3$, the balance becomes as follows:

$$C(\mathscr{R}) = C_{\mathrm{R}} + \frac{K_0\mathscr{R}^3}{3RD}. \tag{5.82}$$

Assuming that $C(\mathscr{R}) \gg C_{\mathrm{R}}$ in Eq. (5.80) and replacing $C(\mathscr{R})$ by C, we obtain the total rate of diffusion-controlled absorption of point defects by the void by multiplying Eq. (5.80) by the number of voids per unit volume ρ_{V}:

$$\text{Rate of absorption/cm}^3 = 4\pi RD\rho_{\mathrm{V}}C. \tag{5.83}$$

The rate constant for diffusion-controlled reaction of point defects and a perfect spherical sink of radius R is then:

$$\begin{aligned} K_{\mathrm{iV}} &= 4\pi RD_{\mathrm{i}}, \\ K_{\mathrm{vV}} &= 4\pi RD_{\mathrm{v}}, \\ k_{\mathrm{V}}^2 &= 4\pi R\rho_{\mathrm{V}}, \end{aligned} \tag{5.84}$$

where the subscripts on K refer to the reacting species, vacancies or interstitials (v, i), and voids V.

5.5.2 *Defect–Dislocation Reactions*

Diffusion-controlled reactions between defects and dislocations occur in much the same way as in the case of spherical sinks, but in cylindrical coordinates. Taking the

capture radius of the sink to be R_d and the dislocation density to be ρ_d, we define the unit cell such that:

$$(\pi \mathscr{R}^2)\rho_d = 1. \tag{5.85}$$

The diffusion equation is given as:

$$\frac{D}{r}\frac{d}{dr}\left(r\frac{dC}{dr}\right) + K_0 = 0, \tag{5.86}$$

with boundary conditions:

$$C(R_d) = C_{Rd} \tag{5.87}$$

$$\left(\frac{dC}{dr}\right)_{\mathscr{R}} = 0, \tag{5.88}$$

and solution:

$$C(r) = C_{R_d} + \frac{K_0\mathscr{R}^2}{2D}\left[\ln\left(\frac{r}{R_d}\right) - 1/2\left(\frac{r^2 - R_d^2}{\mathscr{R}^2}\right)\right]. \tag{5.89}$$

Analogous to the case for spherical sinks in region 1, but in cylindrical geometry instead, the diffusion equation is given as:

$$\frac{1}{r}\frac{d}{dr}\left(r\frac{dC}{dr}\right) = 0, \tag{5.90}$$

with boundary conditions:

$$C(R_d) = C_{Rd} \tag{5.91}$$

$$C(\mathscr{R}) = C, \tag{5.92}$$

with solution:

$$C(r) = C_{R_d} + [C(\mathscr{R}) - C_{R_d}]\frac{\ln(r/R_d)}{\ln(\mathscr{R}/R_d)}. \tag{5.93}$$

The flux of defects to the dislocation line is given as:

$$J = -D\left(\frac{dC}{dr}\right)_{R_d} = \frac{-D[C(\mathscr{R}) - C_{R_d}]}{R_d \ln(\mathscr{R}/R_d)}. \tag{5.94}$$

The absorption rate per unit length of dislocation line = $-(2\pi R_d)J$

$$= \frac{2\pi D[C(\mathscr{R}) - C_{R_d}]}{\ln(\mathscr{R}/R_d)}. \tag{5.95}$$

The rate of defect production in the capture volume

$$= \pi(\mathscr{R}^2 - R_d^2)K_0, \tag{5.96}$$

and since all defects produced in the capture volume are captured by the dislocation:

$$\frac{2\pi D[C(\mathscr{R}) - C_{R_d}]}{\ln(\mathscr{R}/R_d)} = \pi(\mathscr{R}^2 - R_d^2)K_0, \tag{5.97}$$

and

$$C(\mathscr{R}) = C_{R_d} + \frac{K_0\mathscr{R}^2}{2D}\ln(\mathscr{R}/R_d) \qquad \text{for } R_d/\mathscr{R} \ll 1, \tag{5.98}$$

so from Eq. (5.94) the rate of defect capture by dislocations per unit volume = $\dfrac{2\pi D\rho_d C}{\ln(\mathscr{R}/R_d)}$, and the rate constants for vacancies and interstitials are as follows:

$$\begin{aligned} K_{vd} &= \frac{2\pi D_v}{\ln(\mathscr{R}/R_{vd})} \\ K_{id} &= \frac{2\pi D_i}{\ln(\mathscr{R}/R_{id})}, \end{aligned} \tag{5.99}$$

and

$$\begin{aligned} k_{vd}^2 &= \frac{2\pi\rho_d}{\ln(\mathscr{R}/R_{vd})} \\ k_{id}^2 &= \frac{2\pi\rho_d}{\ln(\mathscr{R}/R_{id})}. \end{aligned} \tag{5.100}$$

Note that the combinatorial factors for vacancies and interstitials differ by the capture radius. The capture radius for interstitials is slightly greater than that for vacancies and is the origin of the dislocation bias for interstitials.

5.6 Mixed Rate Control

Mixed rate control occurs when the reaction rate is determined by a combination of processes. We can determine the rate constant for the combined processes by adding the reciprocals of the rate constants to give the resistance due to series steps of diffusion and surface attachment. For the case of voids, we use the rate constants given by Eqs. (5.65) and (5.84) giving:

$$\frac{1}{K_{\text{eff}}} = \frac{1}{K_{\text{reaction}}} + \frac{1}{K_{\text{diffusion}}}, \tag{5.101}$$

to yield the effective rate constant:

$$K_{\text{eff}} = \frac{4\pi RD}{1+\dfrac{a}{R}}, \quad k^2_{\text{eff}} = \frac{4\pi R\rho_{\text{V}}}{1+\dfrac{a}{R}}. \tag{5.102}$$

For large spheres, $a/R \rightarrow 0$ and the rate constant is that for diffusion only. This result shows that reaction rate limitations to capture kinetics for spherical sinks are only significant if the sphere radius is small, approaching the lattice constant.

For dislocations, the capture rates calculated from a diffusion-controlled process verses a reaction rate-controlled process are as follows:

$$\begin{aligned} K_{\text{diffusion}} &= \frac{2\pi D}{\ln(\mathscr{R}/R_{\text{d}})} \\ K_{\text{reaction}} &= z_{\text{d}} D, \end{aligned} \tag{5.103}$$

giving the effective rate constant for mixed-control:

$$K_{\text{eff}} = \frac{D}{\dfrac{1}{z_{\text{d}}} + \dfrac{\ln(\mathscr{R}/R_{\text{d}})}{2\pi}}, \quad k^2_{\text{eff}} = \frac{\rho_{\text{d}}}{\frac{1}{z_{\text{d}}} + \dfrac{\ln(\mathscr{R}/R_{\text{d}})}{2\pi}} \tag{5.104}$$

Consider z_{d} to be the area of a circular region of radius R_{d} multiplied by the number of atoms per unit area. For the (100) plane of the fcc lattice, the number of atoms/unit area is $2/a^2$ and:

$$K_{\text{reaction}}/D = z_{\text{d}} = \frac{2\pi R_{\text{d}}^2}{a^2} = 24 \qquad \text{for } R_{\text{d}} \sim 0.6\,\text{nm and } a \sim 0.3\,\text{nm}. \tag{5.105}$$

For a dislocation line density of 10^{10} cm^{-2}, $K_{\text{diffusion}}/D = \dfrac{2\pi}{\ln(\mathscr{R}/R_{\text{d}})} = 1.4$. So capture of defects by dislocations is diffusion-controlled.

5.7 Defect–Grain Boundary Reactions

Interactions between point defects and grain boundaries are important in the case of radiation-induced segregation, discussed in Chap. 6. Following the analysis of Heald and Harbottle [9], the sink strength of the grain boundary is determined by considering a spherical grain of radius a, with grain boundary defect concentration equal to the thermal equilibrium value, which will be neglected compared to the irradiated-induced concentration. The loss to sinks within the grain is given as:

$$k^2DC = (z_d\rho_d + 4\pi R_V\rho_V)DC, \tag{5.106}$$

where k^2 is the sink strength for the grain interior due to dislocations and voids, and the diffusion equation is given as:

$$\frac{d^2C}{dr^2} + \frac{2}{r}\frac{dC}{dr} + \frac{K_0}{D} - k^2C = 0, \tag{5.107}$$

subject to boundary conditions $C(r = a) = 0$ and $C(r = 0) =$ finite. The solution to Eq. (5.107) subject to the boundary conditions is given as:

$$C(r) = \frac{K_0}{Dk^2}\left[1 - \frac{a\ \sinh(kr)}{r\ \sinh(ka)}\right], \tag{5.108}$$

and the total flow of point defects to the grain boundary, A, is given as:

$$A = -4\pi r^2 D\frac{\partial C}{\partial r}\bigg|_{r=a} = \frac{4\pi K_0 a}{k^2}[ka\ \cot(ka) - 1]. \tag{5.109}$$

Written in rate theory formalism, Eq. (5.109) becomes as follows:

$$A = z_{gb}DC_0, \tag{5.110}$$

where z_{gb} is the sink strength for an individual grain boundary and C_0 is the concentration at the grain center ($r = 0$), Fig. 5.13:

$$C_0 = C(r = 0) = \frac{K_0}{Dk^2}\left[1 - \frac{ka}{\sinh(ka)}\right]. \tag{5.111}$$

From Eqs. (5.109), (5.110), and (5.111), the grain boundary sink strength, z_{gb}, is given as:

$$z_{gb} = 4\pi a\left[\frac{ka\ \cosh(ka) - \sinh(ka)}{\sinh(ka) - ka}\right]. \tag{5.112}$$

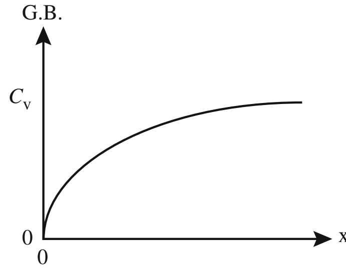

Fig. 5.13 Diffusion-controlled reaction between vacancies and a grain boundary

For small grains and low sink strengths, $ka \rightarrow 0$, and:

$$z_{gb}(ka \to 0) = 8\pi a = 4\pi d, \tag{5.113}$$

where $d(=2a)$ is the grain diameter. When the sink strength is large, $ka \rightarrow \infty$, and:

$$z_{gb}(ka \to \infty) = 4\pi k a^2 = \pi k d^2. \tag{5.114}$$

The grain boundary sink strength is the product of z_{gb} and the grain density in grains per unit volume, or $\rho_{gb} = 6/\pi d^3$, giving:

$$k_{gb}^2(ka \to 0) = 24/d^2, \quad K_{jgb} = 4\pi D_j d, \tag{5.115}$$

and

$$k_{gb}^2(ka \to \infty) = 6k/d, \quad K_{jgb} = \pi k D_j d^2, \tag{5.116}$$

where j = i or v.

Generally, $k^2 \sim 10^{11}$ cm^{-2} and $d > 10^{-3}$ cm so that Eq. (5.116) is the appropriate expression for the grain boundary sink strength. In fact, the grain boundary sink strength is given by Eq. (5.116) whenever $(z_d\rho_d + 4\pi R_V\rho_V) > 1/d$.

5.8 Coherent Precipitates and Solutes

These types of sinks are known as variable bias sinks in that they act as traps for vacancies and interstitials rather than as infinite sinks, in which the defect loses its identity after being absorbed. The source of the attraction of vacancies and interstitials to the trap is the relief of the strain field produced by the coherency between

the trap and the lattice. The coherent precipitate is of a structure in which the lattice planes of the precipitate are continuous with those of the matrix, but due to the difference in lattice parameters, there is a strain field at the interface where the lattice planes from each are forced to match. The over- or undersized solute is a limiting case of a coherent precipitate. The trap strength is limited by the capacity of the interface to hold or trap a defect until the anti-defect arrives and results in annihilation. Hence, no matter accumulates at this defect and thermal emission does not occur. The interface does exhibit a bias for defects and this bias is a function of the biased sinks in the solid. For example, if the biased sinks in the solid favor interstitials, then $k_i^2 > k_v^2$ and the trap interface will acquire slightly more vacancies than interstitials. This excess of vacancies then causes the trap surface to become a more effective sink for interstitials than for vacancies. The biases for the trap are denoted by Y_v and Y_i (Brailsford and Bullough [10] and Olander [3] provide detailed analyses of the bias factors), and the absorption rates of vacancies and interstitials at the trap are given by:

$$\begin{aligned} A_v^{CP} &= 4\pi R_{CP} D_v C_v \rho_{CP} Y_v = K_{vCP} C_v \rho_{CP} \\ A_i^{CP} &= 4\pi R_{CP} D_i C_i \rho_{CP} Y_i = K_{iCP} C_i \rho_{CP}. \end{aligned} \tag{5.117}$$

If there can be no steady-state accumulation of defects at the trap, then there is no net matter flow to or from the sinks and:

$$4\pi R_{CP} \rho_{CP} D_v C_v Y_v = 4\pi R_{CP} \rho_{CP} D_i C_i Y_i, \tag{5.118}$$

so

$$Y_i = \frac{D_v C_v}{D_i C_i} Y_v, \tag{5.119}$$

and the rate constants and sink strengths are as follows:

$$\begin{aligned} K_{vCP} &= 4\pi R_{CP} D_v Y_v; \quad k_{vCP}^2 = 4\pi R_{CP} \rho_{CP} Y_v \\ K_{iCP} &= 4\pi R_{CP} D_i Y_i; \quad k_{iCP}^2 = 4\pi R_{CP} \rho_{CP} Y_i. \end{aligned} \tag{5.120}$$

So variable bias sinks play an interesting role in that they adjust their preference for point defects in response to the relative sink strengths in the bulk.

The reaction rate constants for the various reactions are summarized in Table 5.2 for the various defect–defect and defect–sink reactions.

Table 5.2 Reaction rate constants for defect–sink reactions

Reaction	Rate constant	Sink strength	Eq. #
v + v	$K_{2\mathrm{v}} = \frac{z_{2\mathrm{v}}\Omega D_{\mathrm{v}}}{a^2}$	–	Equation (5.58)
i + i	$K_{2\mathrm{i}} = \frac{z_{2\mathrm{i}}\Omega D_{\mathrm{i}}}{a^2}$	–	Equation (5.58)
v + i	$K_{\mathrm{iv}} = \frac{z_{\mathrm{iv}}\Omega D_{\mathrm{i}}}{a^2}$	–	Equation (5.61)
v, i + void			
Reaction rate control	$K_{\mathrm{vV}} = \frac{4\pi R^2 D_{\mathrm{v}}}{a} \quad K_{\mathrm{iV}} = \frac{4\pi R^2 D_{\mathrm{i}}}{a}$	$k^2_{\mathrm{vV}} = k^2_{\mathrm{iV}} = \frac{4\pi R^2 \rho_V}{a}$	Equation (5.65)
Diffusion control	$K_{\mathrm{vV}} = 4\pi R D_{\mathrm{v}} \quad K_{\mathrm{iV}} = 4\pi R D_{\mathrm{i}}$	$k^2_{\mathrm{vV}} = k^2_{\mathrm{iV}} = 4\pi R \rho_{\mathrm{V}}$	Equation (5.84)
Mixed rate control	$K_{\mathrm{vV}} = \frac{4\pi R D_{\mathrm{v}}}{1 + \frac{a}{R}} \quad K_{\mathrm{iV}} = \frac{4\pi R D_{\mathrm{i}}}{1 + \frac{a}{R}}$	$k^2_{\mathrm{vV}} = k^2_{\mathrm{iV}} = \frac{4\pi R \rho_{\mathrm{V}}}{1 + \frac{a}{R}}$	Equation (5.102)
v, i + dislocation			
Diffusion control	$K_{\mathrm{vd}} = \frac{2\pi D_{\mathrm{v}}}{\ln(\mathscr{R}/R_{\mathrm{vd}})} \quad K_{\mathrm{id}} = \frac{2\pi D_{\mathrm{i}}}{\ln(\mathscr{R}/R_{\mathrm{id}})}$	$k^2_{\mathrm{vd}} = \frac{2\pi \rho_d}{\ln(\mathscr{R}/R_{\mathrm{vd}})} \quad k^2_{\mathrm{id}} = \frac{2\pi \rho_{\mathrm{d}}}{\ln(\mathscr{R}/R_{\mathrm{id}})}$	Equations (5.99, 5.100)
Reaction rate control	$K_{\mathrm{vd}} = z_{\mathrm{vd}} D_{\mathrm{v}} \quad K_{\mathrm{id}} = z_{\mathrm{id}} D_{\mathrm{i}}$	$k^2_{\mathrm{vd}} = z_{\mathrm{vd}} \rho_{\mathrm{d}} \quad k^2_{\mathrm{id}} = z_{\mathrm{id}} \rho_{\mathrm{d}}$	Equation (5.67)
Mixed rate control	$K_{\mathrm{vd}} = \frac{D_{\mathrm{v}}}{\frac{1}{z_{\mathrm{vd}}} + \frac{\ln(\mathscr{R}/R_{\mathrm{vd}})}{2\pi}} \quad K_{\mathrm{id}} = \frac{D_{\mathrm{i}}}{\frac{1}{z_{\mathrm{id}}} + \frac{\ln(\mathscr{R}/R_{\mathrm{id}})}{2\pi}}$	$k^2_{\mathrm{vd}} = \frac{\rho_{\mathrm{d}}}{\frac{1}{z_{\mathrm{vd}}} + \frac{\ln(\mathscr{R}/R_{\mathrm{vd}})}{2\pi}} \quad k^2_{\mathrm{id}} = \frac{\rho_{\mathrm{d}}}{\frac{1}{z_{\mathrm{id}}} + \frac{\ln(\mathscr{R}/R_{\mathrm{id}})}{2\pi}}$	Equation (5.104)
v, i + grain boundary			
Diffusion control	$K_{\mathrm{vgb}} = 4\pi D_{\mathrm{v}} d \quad K_{\mathrm{igb}} = 4\pi D_{\mathrm{i}} d$ $K_{\mathrm{vgb}} = \pi k D_{\mathrm{v}} d^2 \quad K_{\mathrm{igb}} = \pi k D_{\mathrm{i}} d^2$	$k^2_{\mathrm{gb}} = 24/d^2, \quad d < 10^{-3}$ cm $k^2_{\mathrm{gb}} = 6k/d, \quad d > 10^{-3}$ cm	Equation (5.115) Equation (5.116)
v, i + coherent ppt	$K_{\mathrm{vCP}} = 4\pi R_{\mathrm{CP}} D_{\mathrm{v}} Y_{\mathrm{v}}, \quad K_{\mathrm{iCP}} = 4\pi R_{\mathrm{CP}} D_{\mathrm{i}} Y_{\mathrm{i}}$	$k^2_{\mathrm{vCP}} = 4\pi R_{\mathrm{CP}} \rho_{\mathrm{CP}} Y_{\mathrm{v}}, \quad k^2_{\mathrm{iCP}} = 4\pi R_{\mathrm{CP}} \rho_{\mathrm{CP}} Y_{\mathrm{i}}$	Equation (5.120)

5.9 Point Defect Recovery

When irradiated materials are annealed, they exhibit stages, or temperature regimes, that correspond to the loss of defects by mutual annihilation or by diffusion to sinks. Experimental studies use isochronal annealing followed by electrical resistivity at low temperature to identify the major defect recovery processes. Irradiation and electrical resistivity measurements are conducted at low temperature (e.g., 4 K) where defects are immobile and thermal scattering contributions to resistivity are minimal. The appearance of any given stage depends on the time and temperature used in the annealing experiment, and often on the time and temperature of irradiation. Therefore, they are not precisely defined.

Since electrical resistivity is proportional to the total concentration of all irradiation-produced point defects, the resistivity increase per unit irradiation dose is therefore a measure of the concentration of stable defects produced at a given irradiation temperature. Measurements of the change in electrical resistivity, $\Delta\rho$, as a function of annealing temperature provide information on the kinetics of defect reactions. For example, if recombination of vacancies and interstitials occurs, a decrease of $\Delta\rho$ with temperature follows. Figure 5.14 shows a plot of the fractional change in defect concentration ($\Delta\rho/\Delta\rho_0$ is proportional to N/N_0) as a function of temperature in pure copper after electron irradiation at 4 K. Note that there are five major stages of annealing.

Based on the one-interstitial model, Stage I corresponds to the onset of SIA migration. In fact, Stage I consists of five substages, I_A–I_E, as shown in Fig. 5.15. Details of Stage I annealing of copper are shown in Table 5.3. The lower temperature substages, I_A, I_B, and I_C, are due to collapse of close Frenkel pairs. That is, recombination of vacancy–interstitial pairs that were not created far enough away from each other to escape the attractive forces and thus the interstitial recombines with its vacancy counterpart. The differences between stages I_A, I_B, and I_C may be due to alternative interstitial structures or to directions of separation in the lattice.

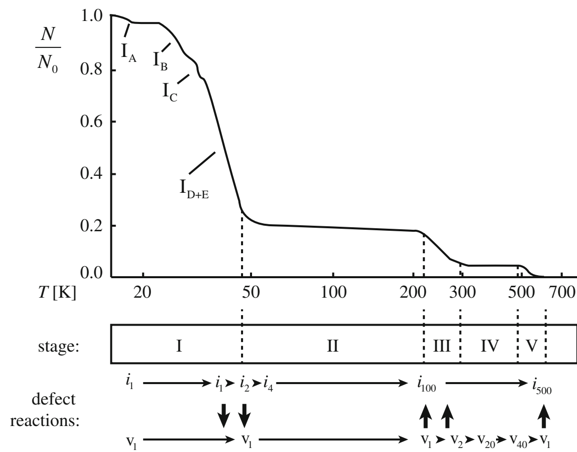

Fig. 5.14 Annealing stages and defect reactions in pure copper after electron irradiation; i_1 and v_1 denote single interstitials and vacancies, respectively, i_2 and v_2 di-interstitials and divacancies (after [11])

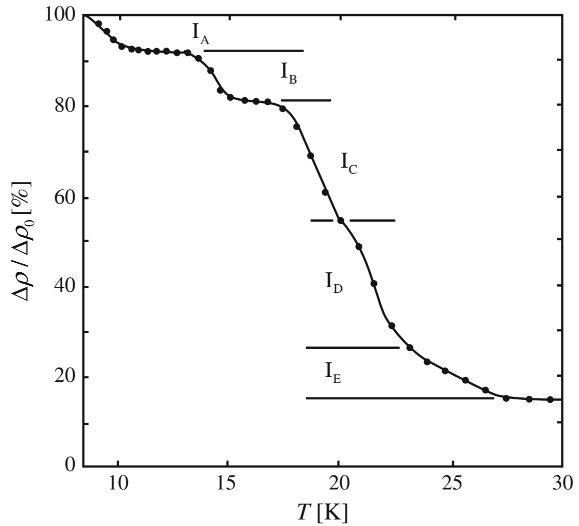

Fig. 5.15 Isochronal annealing curves of a Pt sample irradiated at 4.5 K with 3 MeV electrons to $\Delta\rho_0 = 4 \times 10^{-9}\ \Omega$ cm. Isochronal holding times were 20 min for temperature steps of $\Delta T/T = 3.5$ % (after [11])

Table 5.3 Stage 1 annealing of copper (after [12])

	I_A	I_B	I_C	I_D	I_E
Temperature (K)	16	28	32	39	53
Activation energy (eV)	0.05	0.085	0.095	0.12	0.12
Reaction order	1	1	1	1	1
Number of jumps	1	1	1	10	10^4
Impurity effect	–	Small reduction	–	Large reduction	Large reduction
Dose effect	–	–	–	–	Moves to lower T
Increasing e^- energy	Increase		Reduce		Increase

Stages I_D and I_E are due to recombination by long-range migration of interstitials. Stage I_D is due to correlated recombination in which the interstitial atom recombines with the vacancy created by the same displacement event. Stage I_E is due to uncorrelated recombination of an interstitial with a vacancy from a different displacement event. In these cases, recovery may consist of tens or hundreds of jumps. Stages I_D and I_E are observed when the Frenkel pair density is small enough so that the average distance of an interstitial atom to a vacancy from a different displacement event is much larger than that to a vacancy from the same displacement event. Note that interstitial clustering occurs simultaneously with recombination and is responsible for the survival of interstitials at the end of Stage I and for the incompleteness of recovery in this stage.

Stage II recovery describes migration and growth of small interstitial clusters and SIA-impurity clusters and occurs in the temperature range 50–200 K in copper. The

minimal change in resistivity of Stage II is indicative of the importance of impurities in this stage. Impurities can trap interstitials, delaying interstitial clustering reactions. Stage II is more prominent in impure materials or when pure materials are doped with impurities that could form SIA-impurity clusters.

In Stage III, vacancies migrate and annihilate at interstitial clusters. Vacancy migration also results in vacancy agglomeration and at the end of Stage III, surviving defects consist of small vacancy clusters and larger interstitial loops. Vacancy clusters grow in Stage IV to such a size that they are visible in the transmission electron microscope as small voids. Impurities may affect vacancy clustering and alter Stage IV recovery. Stage V corresponds to the thermal dissociation of vacancy clusters followed by vacancy annihilation at interstitial loops such that at the end of stage V all damage is removed.

The specific processes that occur after Stage III are less well defined for several reasons. For a number of metals (Al, Pt, Au), recovery is complete after Stage III since the loss of mobile vacancies to interstitial clusters is apparently so great that the residual vacancy clusters are not large enough to survive Stage III. Multiple-defect structures are not easily formed by electron irradiation and so stages IV and V are rather ill-defined. Defect clusters are more readily formed by neutron or ion irradiation that produce large defect cascades in which separation of the vacancy core from the interstitial shell enhances agglomeration reactions. In this case, a much larger fraction of vacancies and interstitials survive Stage I and Stage III, respectively. It also means that annealing behavior is dependent on the irradiating particle. Further, the wide range of cluster geometries that can nucleate and evolve make for a very complex microstructure with many recovery pathways.

Nomenclature

A	Flow rate of defects to sink
a	Lattice constant, also grain radius
C	Concentration
C_{giL}	Mobile SIA cluster concentration
C_{iv}	Interstitial, vacancy concentration
C_{R}	Vacancy concentration at void boundary
C_{s}	Sink concentration
d	Grain diameter
D_{rad}	Radiation-enhanced diffusion coefficient
D_{th}	Thermal diffusion coefficient
D_{m}	Ballistic mixing diffusion coefficient
D_0^y	Pre-exponential factor in the diffusion coefficient via defect y
D_x^y	Diffusion coefficient for species x via y
E_{m}^y	Migration energy of defect y
f	Correlation coefficient
i	Interstitial
v	Vacancy
s	Sink

J_x Flux of atom or defect x across a marker plane
k Boltzmann's constant
k_{jX}^2 Strength of sink X for defect j
K_0 Defect production rate
K_{gb} Rate constant for defect–grain boundary interaction
K_{g} Rate constant for interstitial interaction with glissile SIA loops
K_{giL} Production rate of glissile interstitial loops
K_{id} Rate constant for interstitial–dislocation interaction
K_{iv} Vacancy–interstitial recombination rate constant
K_{is} Interstitial–sink reaction rate constant
K_{vd} Rate constant for vacancy–dislocation interaction
K_{vs} Vacancy–sink reaction rate constant
$K_{2\mathrm{v}}$ Divacancy formation rate constant
L_{v} Thermal vacancy production term
N Atom fraction
r_{iv} Vacancy–interstitial recombination radius
r_{is} Interstitial–sink recombination radius
r_{vs} Vacancy–sink recombination radius
p Sink annihilation probability
$P_{2\mathrm{v}}$ Probability/second of forming a divacancy
P_x Probability/second that a vacancy jumps to a nearest neighbor to a vacancy
R_{d} Dislocation core radius
R_{id} Reaction rate between interstitials and dislocations
R_{vd} Reaction rate between vacancies and dislocations
$R_{2\mathrm{v}}$ Rate of divacancy formation
$\mathscr{R}$ Radius of unit cell or capture volume surrounding a spherical sink
t Time
T Temperature
T_{c} Critical temperature defined by Eq. (5.50)
v_2 Divacancy designation
z_{gb} Sink strength for an individual grain boundary
z_{xy} Combinatorial number for a reaction between x and y
$\varepsilon_{\mathrm{i,v}}$ Fraction of clustered interstitials, vacancies
ε_{r} Fraction of defects recombining in cascade
ϕ Particle flux
ρ_{d} Dislocation density
η Parameter defined by Eq. (5.45)
σ_{s} Microscopic scattering cross section
τ_x Time constant for process x
ω Jump frequency
Ω Atomic volume
ξ Production efficiency term

Subscripts

a Atoms
CP Coherent precipitate
d Dislocation
g Glissile
gb Grain boundary
giL Glissile interstitial loop
i,v Interstitials, vacancies
m Migration
Rad Under irradiation
r Recombination
R Void radius
s Sink
V Void

Superscripts

i, v Interstitials, vacancies

Problems

5.1 Point defect concentration buildup during irradiation can be described by:

$$\frac{dC_v}{dt} = K_0 - K_{iv}C_iC_v - K_{vs}C_vC_s + \nabla \cdot (D_v \nabla C_v)$$
$$\frac{dC_i}{dt} = K_0 - K_{iv}C_iC_v - K_{is}C_iC_s + \nabla \cdot (D_i \nabla C_i)$$

How do these equations simplify if you are irradiating a single crystal with no defects present? In that case, what is the relationship between vacancy and interstitial concentrations? Do the vacancy and interstitial concentrations differ if you start with a sample that contains defects?

5.2 For pure nickel irradiated at 500 °C:

(a) Calculate the steady-state concentration of vacancies and interstitials.

$$K_0 = 5 \times 10^{-4}\,\text{dpa/s} \quad \Delta H_m^v = 0.82\,\text{eV}$$
$$C_s = 10^9\,\text{cm}^{-3} \quad \Delta H_m^i = 0.12\,\text{eV}$$
$$r_{iv} = r_{is} = r_{vs} = 10a \quad \Delta S_m^v = \Delta S_m^i = 0$$
$$\nu = 10^{13}\,\text{s}^{-1} \quad a = 0.352\,\text{nm}$$

(b) For a dislocation density of 10^{12} cm^{-2}, determine the temperature at which mutual recombination gives way to annealing at fixed sinks.

5.3 A perfect, single crystal Cu wire (cylinder) of radius R = 10 nm and length $L \gg R$ is irradiated at 400 °C. The only sink present is the surface.

(a) Assuming negligible recombination, solve the diffusion equation:

$$\frac{\partial C_x}{\partial t} = K_0 + D_x \nabla^2 C_x$$

at steady state for x = interstitial or vacancy, to obtain the vacancy and interstitial concentration profiles. What boundary condition do you use at the surface? When you solve the equation pay attention to the symmetry of the problem to eliminate terms in the expression for $\nabla^2 C_x$.

(b) Calculate the rates of absorption (number of defects per unit area and time) at the surface.

(Hint: remember that $\nabla^2 C$ is continuous.)

5.4 Calculate the steady-state radiation-enhanced diffusion coefficient for copper at T/T_m = 0.5 in terms of K_0, the defect production rate, and ρ_d, the dislocation sink density.

5.5 Assume for a metal of interest that the interstitial–sink interaction radius and the vacancy–sink interaction radius are equal. Two irradiations are performed at low, but non-negligible sink density. The displacement rate is the same for both irradiations. In the second irradiation, a minor alloying addition doubles the diffusion coefficient of interstitials but does not change the diffusion coefficient for vacancies. By how much does the ratio of the steady-state vacancy to interstitial concentrations change? Explain physically what happens to the point defects.

5.6 A sample of aluminum is held at room temperature (20 °C) and irradiated with a monoenergetic beam of 1 MeV neutrons at a flux of 10^{14} n/cm^{2}s. Assume that the capture radii $r_{iv} = r_{is} = r_{vs}$ are all approximately 10a.

(a) At what sink density does defect annihilation at sinks overtake mutual recombination?

(b) What is the value of the radiation-enhanced steady-state diffusion coefficient of aluminum atoms? How does this compare to the diffusion coefficient in the absence of irradiation?

(c) Verify that your calculations in part (b) do indeed represent a steady-state condition, i.e., $dC_v/dt = dC_i/dt = 0$.

5.7 A defect-free Al crystal is irradiated at a displacement rate of 10^{-5} dpa/s.

(a) Calculate the steady-state concentration of point defects at T = 100 °C and 500 °C.

(b) Once steady state is reached, the irradiation is stopped. Calculate the time constant for recombination as a function of temperature.

(c) One wishes to measure the defect concentration in the irradiated Al, a process assumed to take 100 s. Determine the temperature range for which the defect concentration can be kept within 1 % of its value at the end of the irradiation for this length of time.
Assume the combinatorial factor, $z = 500$.

5.8 Following the analysis for the diffusion rate of point defects to spherical sinks, derive an expression for the vacancy concentration profile around a dislocation. What is the vacancy capture rate by dislocations?

5.9 For fcc nickel, determine whether vacancy capture by dislocations is a diffusion-controlled or reaction rate-controlled process. What about interstitial capture by dislocations?

z_d Area of the circular region about the dislocation (defined by the capture radius) multiplied by the number of atoms per unit area
r_{vd} Capture radius for vacancies = 0.6 nm
r_{id} Capture radius for interstitials = 0.7 nm
ρ_d 10^{10} cm^{-2}

5.10 It can be shown that the time constant (characteristic time) for the process v + s → s is $\tau_3 = (K_{vs}C_s)^{-1}$. At sufficiently high temperature, vacancies may be mobile so that the reaction v + v → v_2 may terminate the increase in vacancy concentration with time. If the consumption rate of vacancies in divacancy formation is $K_{vv}C_v^2$, determine the time constant for the onset of steady state.

5.11 A sample of fcc copper with a low sink density ($\tau_1 < \tau_2$) is irradiated at low temperature ($T/T_m = 0.3$) until steady state is reached. Some time later, all sinks instantly disappear and a new steady state is reached. Determine the magnitude of the change in C_v and C_i between the two steady states.

5.12 Explain the reason (or likely reasons) for the following observations:

(a) The displacement rate at the surface of a copper sample is 1000 times higher when irradiated with 1 MeV Cu^+ ions than with 1 MeV protons at the same flux.
(b) A scattering experiment using 3 MeV B^+ ions on Cu produces yields that disagree sharply with calculations using the Rutherford scattering formula.
(c) A single crystal of copper is irradiated with 2 MeV He^+ ions and the backscatter yield is only 5 % of that of a polycrystal.
(d) Irradiation of a metal with a high neutron flux does not produce a measurable increase in the atom diffusion coefficient.
(e) Two metals are pressed together and heated to $0.5T_m$. It is observed that atoms from the metals intermix at the interface. Attempts to determine the defect(s) responsible for the intermixing reveal that vacancies account for 100 % of the atom mixing. True or false? Why?

5.13 Two engineers are arguing over how to test the effect of the high point defect concentration developed during irradiation on the deformation rate of nickel at 500 °C. Engineer #1 maintains that one can irradiate the sample to the appropriate fluence at the temperature of interest, remove it from the reactor, and heat it back up to temperature to perform the test. Engineer #2 insists that the concentration of point defects decays almost immediately after irradiation ceases and therefore, tests must be performed in situ. Who is right? Why? (Hint: consider the point defect equation for the slowest defect (vacancy) only, neglect recombination, and consider that the only sinks present are dislocations at a concentration of 10^9 cm^{-2}).

$$D_{\mathrm{v}}^{\mathrm{Ni}}(500\,^{\circ}\mathrm{C}) \sim 10^{-8}\,\mathrm{cm}^2/\mathrm{s}$$
$$a \sim 0.3\,\mathrm{nm}$$

5.14 Assume a solid containing defect sinks is irradiated at a temperature T_0, at which only vacancies are mobile.

(a) For the case of a high sink density, estimate the time, t_1, at which sinks will contribute to interstitial annihilation. Neglect recombination.
(b) For the case of a low sink density, estimate the time, t_2, at which recombination will contribute to vacancy annihilation. Neglect the effect of sinks.
(c) Describe what changes can be made in either the irradiation process or the material microstructure to force $t_1 = t_2$.

Assume a quasi-steady-state condition exists, beginning at t_1 in part (a) and at t_2 in part (b).

5.15 Show that, for a metal with a low sink density undergoing neutron irradiation at low temperature ($T/T_{\mathrm{m}} < 0.2$), when sinks contribute to interstitial annihilation, the vacancy and interstitial concentrations as a function of time can be written as:

$$C_{\mathrm{v}} = (K_0 K_{\mathrm{is}} C_{\mathrm{s}} t / K_{\mathrm{iv}})^{1/2}$$
$$C_{\mathrm{i}} = (K_0 / K_{\mathrm{iv}} K_{\mathrm{is}} C_{\mathrm{s}} t)^{1/2}$$

(Hint: consider this case to be intermediary to the quasi-steady state and steady-state cases such that $\mathrm{d}C_{\mathrm{i}}/\mathrm{d}t < 0$ and $\mathrm{d}C_{\mathrm{v}}/\mathrm{d}t > 0$ and write the point defect balance equations as inequalities.)

5.16 Two bilayer samples with low sink strengths are being irradiated at low temperature as part of a radiation-enhanced diffusion experiment. If the displacement rate of the second sample is five times that of the first sample, what is the difference in the radiation-enhanced diffusion coefficient?

References

1. Rothman SJ (1983) Effects of irradiation and diffusion in metals and alloys. In: Nolfi FV (ed) Phase transformations during irradiation. Applied Science Publisher, New York, pp 189–211
2. Sizmann R (1978) The effect of radiation upon diffusion in metals. J Nucl Mater 69(70):386–412
3. Olander DR (1976) Fundamental aspects of nuclear reactor fuel elements, TID-26711-P1. Technical Information Service, Springfield, VA
4. Lam NQ (1975) J Nucl Mater 56:125–135
5. Woo CH, Singh BN (1990) Phys Stat Sol (b) 159:609
6. Woo CH, Singh BN, Heinisch HL (1991) J Nucl Mater 179–181:951
7. Wiedersich H (1986) In: Johnson RA, Orlov AN (eds) Physics of radiation effects in crystals. Elsevier Science, New York, p 237
8. Matteson S, Roth J, Nicolet M (1979) Rad Eff 42:217–226
9. Heald PT, Harbottle JE (1977) J Nucl Mater 67:229–233
10. Brailsford AD, Bullough R (1972) J Nucl Mater 44:121–135
11. Ehrhart P, Robrock KH, Schober HR (1986) Basic defects in metals. In: Johnson RA, Orlov AN (eds) Physics of radiation effects in crystals. Elsevier Science Publishers, Amsterdam, p 3
12. Agullo-Lopez F, Catlow CRA, Towsend PD (1988) Point defects in materials. Academic Press Inc, San Diego, pp 198–203